remote sensing

MDPI

*Review*

# Selection of the Key Earth Observation Sensors and Platforms Focusing on Applications for Polar Regions in the Scope of Copernicus System 2020–2030

**Estefany Lancheros [1,*], Adriano Camps [1,*], Hyuk Park [1], Pedro Rodriguez [2], Stefania Tonetti [3], Judith Cote [4] and Stephane Pierotti [4]**

1 Universitat Politècnica Catalunya-BarcelonaTech & IEEC, Campus Nord, 08034 Barcelona, Spain; park.hyuk@tsc.upc.edu
2 Thales Alenia Space, 28760 Madrid, (España)Madrid, Spain; pedro.r@thalesaleniaspace.com
3 Deimos Space S.L.U, 28760 Madrid, Spain; stefania.tonetti@deimos-space.com
4 Thales Alenia Space, 06150 Toulouse, France; judith.cote@thalesaleniaspace.com (J.C.); stephane.pierotti@thalesaleniaspace.com (S.P.)
* Correspondence: estefany@tsc.upc.edu (E.L.); camps@tsc.upc.edu (A.C.); Tel.: +34-626-94-2616 (E.L.); +34-627-01-6695 (A.C.)

Received: 13 November 2018; Accepted: 11 January 2019; Published: 17 January 2019

**Abstract:** An optimal payload selection conducted in the frame of the H2020 ONION project (id 687490) is presented based on the ability to cover the observation needs of the Copernicus system in the time period 2020–2030. Payload selection is constrained by the variables that can be measured, the power consumption, and weight of the instrument, and the required accuracy and spatial resolution (horizontal or vertical). It involved 20 measurements with observation gaps according to the user requirements that were detected in the top 10 use cases in the scope of Copernicus space infrastructure, 9 potential applied technologies, and 39 available commercial platforms. Additional Earth Observation (EO) infrastructures are proposed to reduce measurements gaps, based on a weighting system that assigned high relevance for measurements associated to Marine for Weather Forecast over Polar Regions. This study concludes with a rank and mapping of the potential technologies and the suitable commercial platforms to cover most of the requirements of the top ten use cases, analyzing the Marine for Weather Forecast, Sea Ice Monitoring, Fishing Pressure, and Agriculture and Forestry: Hydric stress as the priority use cases.

**Keywords:** Earth Observation; satellite; sensors; platform; radiometer; SAR; GNSS-R; VIS/NIR imager; polar; weather; ice; marine

## 1. Introduction

The Copernicus system, previously known as Global Monitoring for Environmental Security (GMES), is a revolutionary program of the European Union (EU) to address the end-user requirements over six thematic services: Atmosphere, Marine, Land, Climate Change, Emergency Management, and Security. Copernicus is supported by the space and in situ components. The space segment is based on a set of Earth Observation (EO) satellites known as the Sentinels and some contributing missions. Contributing missions with space infrastructure are the Earth Explorer missions [1] operated by the European Space Agency (ESA), the meteorological missions operated by the European Organization for the Exploitation of Meteorological Satellites (EUMETSAT), and EO missions operated by the European Union (EU), third countries, and commercial providers.

Currently, there are seven Sentinels satellites in orbit: Sentinel-1A and Sentinel-1B with C-band Synthetic Aperture Radar (SAR) for land and ocean observation, Sentinel-2A and Sentinel-2B with high resolution optical imager called Multi-Spectral Imager (MSI) for land and vegetation observation, Sentinel-3A and Sentinel-3B with a suite of instruments such as Synthetic Aperture Radar altimeter (SRAL), and medium resolution optical imager: Ocean and Land Colour Imager (OLCI) and Sea and Land Surface Temperature Radiometer (SLTR) for ocean and land observation, and Sentinel-5P with cross-nadir scanning sounder called Tropospheric Monitoring Instrument (TROPOMI) for atmospheric chemistry and aerosol studies. Future Sentinel missions that will be launched in the next decade are Sentinel-4 for atmospheric chemistry as hosted payload over Meteosat Third Generation-Sounding (MTG-S); Sentinel-5 will be launched as hosted payloads over MetOp-Second generation (MetOp SG) for atmospheric chemistry, aerosol and spectral irradiance studies; and Sentinel-6 will be launched in a Low Earth Orbit (LEO) inclined over the equator for ocean altimetry as an international program between ESA, the National Aeronautics and Space Administration (NASA), the National Centre for Space Studies (CNES), EUMETSAT, and the National Oceanic and Atmospheric Administration (NOAA). Additionally, the third and fourth units of Sentinel-1C/D, Sentinel-2C/D, and Sentinel-3C/D will have planned to launch for the continuity of these programs.

At present, Earth Explorer missions are: Soil Moisture and Ocean Salinity (SMOS) launched on 2 November 2009 for sea surface salinity and soil moisture monitoring; this is considered as a potential gap because this mission has no continuity; Atmospheric Dynamics Mission—Aeolus (ADM-AEOLUS) launched on 22 August 2018, with an Atmospheric Laser Doppler Instrument (ALADIN) for contribution to aerosol observation and wind profile. Future Earth Explorer missions are: EarthCARE mission with a suite of instruments such as a Atmospheric Lidar (ATLID), Broad-Band Radiometer (BBR), Cloud Profiling Radar (CPR), and Multi-Spectral Imager (MSI) for cloud, aerosol, and radiation process studies; Biomass mission with a interferometric and polarimetric P-band SAR for biomass and glacier topography study; and FLEX mission with a FLORIS instrument for photosynthetic activity monitoring. Additionally, the ESA has chosen two potential Earth Explorer candidates missions [2], the Far-infrared Outgoing Radiation Understanding and Monitoring (FORUM) with measure in the 15–100 micron range, and Sea-Surface Kinematics Multi-scale (SKIM) monitoring with a multi-beam radar altimeter with a wide swath. These two candidates considered will spend the next two years being studied thoroughly and only one will be implemented.

State of the art of the meteorological contributing missions of Copernicus are MetOp in Low Earth Orbit (LEO), and Meteosat Second Generation (MSG) in Geostationary orbit (GEO). For the incoming decade (2020 to 2030), these programs will have continuity because new missions will be launched such as Meteosat Third Generation (MTG) and MetOp Second Generation (SG).

For Sentinel expansion, the ESA has identified six possible candidates with phase A/B under preparation for the expansions to the Copernicus space component [3], such as Sentinel-7 Anthropogenic $CO_2$ monitoring mission, Sentinel-8 High Spatio-Temporal Resolution Land Surface Temperature (LST) Monitoring Mission (companion to Sentinel-2 C/D), Sentinel-9 with two components: Polar Ice and Snow Topographic Mission, and Polar Weather payload on a Highly Elliptical Orbit, and Sentinel-10 with a Hyperspectral Imaging Mission. Other possible candidates for the expansion of Copernicus are Passive Microwave Imaging Mission, and L-Band SAR mission. In parallel, a recent study of the Copernicus Market [4] mentioned that the agriculture, ocean monitoring, oil, and gas are a potential market in terms of Copernicus impact and user benefits. The approach followed is to identify the user's needs, identifying the gaps and potential areas for improvement in the Copernicus EO infrastructure, taking into account the future instruments and missions. This form could analyse if the plans of the extension of Copernicus support the emergent needs.

The European Commission (EC) has led a revolutionary programme aiming at securing and exploiting space infrastructure to meet future demands and societal needs. The H2020 Operational Network of Individual Observation Node (ONION) project identified the main needs of the space segment infrastructure of the Copernicus system and identified the key technology challenges to be faced in the future, taking into account the user requirements at the center of the design process. The ONION project analyzed the user needs and ranked the top 10 use cases [5]. Each use case is associated with a Copernicus service, and they are formed by a set of measurements required to meet the users' needs. The measurements are the geophysical products derived from satellite observations. In addition, the measurement gaps and user requirements were identified and defined by the ONION project (Table 1) [5,6], taking into account if, in the coming decade, the Copernicus and contributing missions satisfy the user requirements. This work focuses on the identification of the potential sensor technologies and platforms to meet those needs detected. The capability of the different technologies is evaluated according to current trends in the design of small satellites. These technologies are presented in view of the novel developments in spacecraft and sensor miniaturization, reduced power consumption, measurement requirements, and data quality, in order to cover the user requirements [6], so as to obtain competitive and cost-effectiveness services.

The 20 measurements with gaps detected [6] in the top ten use cases are: (1) Ocean surface currents, (2) dominant wave direction, (3) significant wave height, (4) horizontal wind speed over the sea surface, (5) sea ice type, (6) iceberg tracking, (7) sea ice cover, (8) sea ice extent, (9) sea ice drift, (10) sea ice thickness, (11) atmospheric pressure over the sea surface, (12) sea surface temperature, (13) ocean chlorophyll concentration, (14) ocean imagery and water leaving radiance, (15) color dissolved organic matter, (16) detection of water stress in crops, (17) estimation of crop evapotranspiration, (18) surface soil moisture, (19) crop growth and condition, and (20) monitoring system vessels. Marine for Weather Forecast, Sea Ice Monitoring, Fishing Pressure, and Agriculture and Forestry: Hydric Stress use cases involved all the measurements with observations gaps detected over Copernicus space infrastructure in the period 2020–2030. The Marine for Weather Forecast, Sea Ice Monitoring, and Fishing Pressure use cases are ranked as the emerging observation needs. These use cases required measurements that are of crucial importance for a wide range of activities from maritime traffic, fishery, environment, food and medicine supply for populations at high latitudes, as well as for oil and gas operations. Another high priority use case with observation gaps (Table 1) is the Agriculture and Forestry: Hydric Stress. The key measurements to cover for this use case are important to study the hydrological cycles, agriculture production, climatology, and meteorology. With the objective to cover these 20 measurements with gaps, we designed a methodology that focuses on the critical technologies to complement Copernicus observation gaps.

The methodology applied to select the appropriate sensors and platforms is sketched in Figure 1. First, a survey of the commercial small platform capabilities is presented in terms of mass, payload power, communications, pointing knowledge, and control. Second, the state-of-the-art sensors in terms of mass, power consumption, swath, and data rate is presented. Each sensor or technology is then studied to cover the observation gaps. Based on the survey of the instrument capabilities and data quality, a summary of the existing, and emerging in EO sensors is given, including the scientific and technological limitations in terms of spatial resolution, accuracy, and swath. Within these bounds, the potential instruments are selected according to the available commercial small platforms. The reference instruments are evaluated based on the variables with gaps that can be measured using a scoring method. This scoring method assigns a high score to the sensors that present lower power consumption, lower mass, and high data quality (better accuracy, smaller spatial resolution, and/or wider coverage). Finally, the most relevant instrument technologies compatible with small platforms are identified to complement the existing Copernicus Services for the selected use cases.

**Table 1.** The top ten use cases.

| | Use Case [5] | Copernicus Services Related | 2020–2030 | | |
|---|---|---|---|---|---|
| | | | Copernicus Instrument/Mission [7] | Contributing Instrument/Mission [8] | Measurements with Gaps Detected [6] |
| 1 | Marine for Weather Forecast | Marine | SAR-C/Sentinel-1<br>SRAL/Sentinel-3<br>OLCI/Sentinel-3<br>Poseidon-4/Sentinel-6 | PALSAR-3/ALOS-4<br>SAR-2000 S.G/CSG<br>SAR/HRWS<br>SAR-X/TSX-NG<br>SAR-X/PAZ<br>SWIM/CFOSAT<br>ASCAT/MetOp<br>SCA/MetOp-SG | Wind speed over sea surface (horizontal),<br>Ocean surface currents,<br>Dominant wave direction,<br>Dominant wave period,<br>Significant wave height,<br>Atmospheric pressure over sea surface. |
| 2 | Sea Ice Monitoring: Extent, Thickness | Marine | SAR-C/Sentinel-1<br>SLTR, OLCI, SRAL<br>/Sentinel-3 | PALSAR-3/ALOS-4<br>SAR-2000 S.G/CSG<br>SAR/HRWS<br>SAR-X/TSX-NG<br>SAR-X/PAZ<br>SWIM/CFOSAT<br>ASCAT/MetOp<br>SCA/MetOp-SG<br>MSI/Earth-CARE<br>IASI and AVHRR-3/MetOp<br>METimage,IASI-NG/MetOp-SG | Sea surface temperature,<br>Sea ice cover,<br>Sea ice type,<br>Sea ice thickness,<br>Iceberg tracking,<br>Sea ice drift,<br>Sea ice extent,<br>Wind speed over sea surface horizontal,<br>Ocean surface currents,<br>Dominant wave direction,<br>Dominant wave period,<br>Significant wave height. |
| 3 | Fishing Pressure, Stock Assessment | Marine | OLCI/Sentinel-3<br>SAR-C/Sentinel-1 | SEVERI/MSG<br>MSI/Earth-CARE<br>IASI and AVHRR-3/MetOp<br>METimage,IASI-NG/MetOp-SG<br>FCI/MTG-I<br>IRS/MTG-S<br>FLORIS/FLEX | Color dissolved organic matter,<br>Ocean imagery and water leaving radiance,<br>Ocean chlorophyll concentration,<br>Monitoring system- vessels. |
| 4 | Land for Infrastructure Status Assessment | Security | SAR-C/Sentinel-1<br>MSI/Sentinel-2<br>OLCI/Sentinel-3 | SAR-2000 S.G/CSG<br>SAR-X/TSX-NG<br>HRWS-SAR/HRWS<br>SAR-X/PAZ<br>DESIS/ISS DESIS<br>HYC/PRISMA<br>P-BAND SAR/BIOMASS<br>HSI/EnMap<br>FCI/MTG-I<br>HiRAIS/Deimos-2<br>NAOMI/SPOT-7<br>REIS/RapiEye | None |
| 5 | Agriculture and Forestry: Hydric Stress | Land | SAR-C/Sentinel-1<br>MSI/Sentinel-2<br>SLTR, OLCI/Sentinel-3 | SAR-2000 S.G/CSG<br>SAR-X/TSX-NG<br>HRWS-SAR/HRWS<br>SAR-X/PAZ<br>DESIS/ISS DESIS<br>HYC/PRISMA<br>P-BAND SAR/BIOMASS<br>ASCAT/MetOp<br>SCA/MetOp-SG<br>MSI/EartCARE<br>HSI/EnMap<br>FCI/MTG-I<br>HiRAIS/Deimos-2<br>NAOMI/SPOT-7<br>REIS/RapiEye<br>SEVERI/MSG<br>MSI/Earth-CARE<br>IASI and AVHRR-3/MetOp<br>METimage,IASI-NG/MetOp-SG<br>FCI/MTG-I<br>IRS/MTG-S<br>FLORIS/FLEX | Surface soil moisture,<br>Crop grow and conditions,<br>detection of water stress in crops,<br>Estimation of crop evapotranspiration. |

**Table 1.** *Cont.*

| | Use Case [5] | Copernicus Services Related | 2020–2030 Copernicus Instrument/Mission [7] | Contributing Instrument/Mission [8] | Measurements with Gaps Detected [6] |
|---|---|---|---|---|---|
| 6 | Land for Basic Mapping: Risk Assessment | Emergency Management | SAR-C/Sentinel-1<br>MSI/Sentinel-2<br>OLCI/Sentinel-3 | SAR-2000 S.G/CSG<br>SAR-X/TSX-NG<br>HRWS-SAR/HRWS<br>SAR-X/PAZ<br>DESIS/ISS DESIS<br>HYC/PRISMA<br>P-BAND SAR/BIOMASS<br>HSI/EnMap<br>FCI/MTG-I<br>HiRAIS/Deimos-2<br>NAOMI/SPOT-7<br>REIS/RapiEye | Surface soil moisture. |
| 7 | Sea Ice Melting Emissions Assessment | Marine | SAR-C/Sentinel-1<br>SLTR, OLCI, SRAL/Sentinel-3 | PALSAR-3/ALOS-4<br>SAR-2000 S.G/CSG<br>SAR/HRWS<br>SAR-X/TSX-NG<br>SAR-X/PAZ<br>SWIM/CFOSAT<br>ASCAT/MetOp<br>SCA/MetOp-SG<br>MSI/Earth-CARE<br>IASI and AVHRR-3/MetOp<br>METimage,IASI-NG/MetOp-SG | Sea surface temperature,<br>Sea ice cover,<br>Sea ice type,<br>Sea ice thickness. |
| 8 | Atmosphere for Weather Forecast | Atmosphere | SAR-C/Sentinel-1<br>Sentinel-4/MTG-S<br>Sentinel-5/MetOp-SG<br>TROPOMI/Sentinel-5p | ASCAT/MetOp<br>SCA/MetOP-SG<br>SEVERI/MSG<br>MSI, CPR/Earth-CARE<br>IASI and AVHRR-3/MetOp<br>METimage,IASI-NG/MetOp-SG<br>FCI/MTG-I<br>IRS/MTG-S | Wind speed over sea surface (horizontal),<br>Wind vector over sea surface (horizontal),<br>Atmospheric pressure over sea surface. |
| 9 | Climate for Ozone Layer and UV | Climate Change | SLTR, OLCI/Sentinel-3<br>Sentinel-4/MTG-S<br>Sentinel-5/MetOp-SG<br>TROPOMI/Sentinel-5p | SEVERI/MSG<br>MSI, CPR/Earth-CARE<br>GOME-2, IASI, AVHRR-3/MetOp<br>METimage,IASI-NG/MetOp-SG<br>FCI/MTG-I<br>IRS/MTG-S<br>HYC/PRISMA<br>UVAS/Ingenio | None |
| 10 | Natural Habitat and Protected Species Monitoring | Land | SAR-C/Sentinel-1<br>MSI/Sentinel-2<br>OLCI, SLTR/Sentinel-3<br>Sentinel-4/MTG-S<br>Sentinel-5/MetOp-SG<br>TROPOMI/Sentinel-5p | ASCAT/MetOp<br>SCA/MetOP-SG<br>SEVERI/MSG<br>MSI, CPR/Earth-CARE<br>IASI and AVHRR-3/MetOp<br>METimage,IASI-NG/MetOp-SG<br>FCI/MTG-I<br>IRS/MTG-S<br>HYC/PRISMA<br>FLORIS/FLEX | Surface soil moisture. |

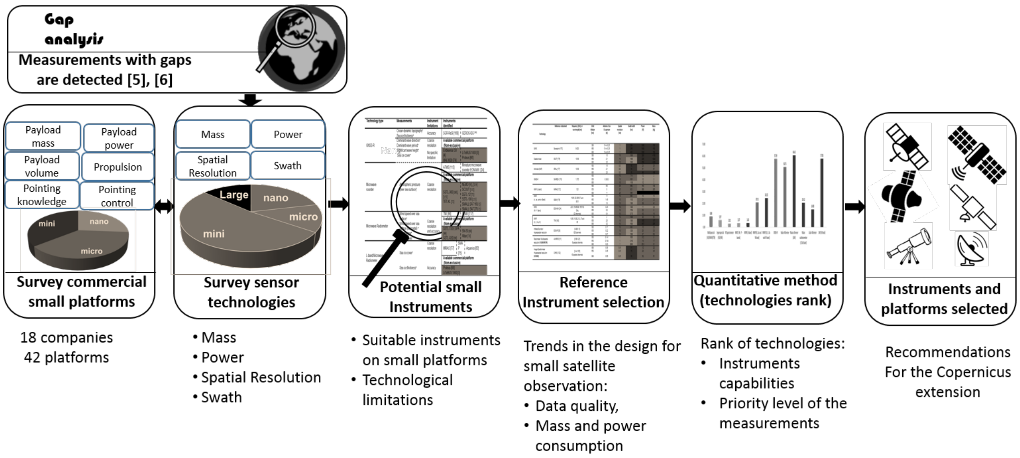


**Figure 1.** Design process to select payload and platform according to the requirements.

## 2. Survey of Commercial Small Platforms

This section presents the results of a comprehensive survey of commercial Low Earth Orbit (LEO) small platforms for EO, in order to properly select the platforms for each technology. To do this, the capabilities and limitations of the small commercial buses are taken into account. A total of forty-two commercial platforms from eighteen different companies have been identified, and their information has been compiled from company websites and conferences proceedings (Appendix A).

These small platforms cover a wide range of payload mass and power. They are categorized into three groups nano-, micro-, and mini-satellites. Table 2 summarizes their typical parameters. These platforms support payload masses from 1 kg to 600 kg [9], payload powers (orbital, average) from 1 W to 1500 W [10], downlink up 15 Mbps (S-band) [11], 100 Mbps (X-band) [12], and 1.2 Gbps (K-band) [13]. In this context, the recent evolution of the capability of micro- and mini-class platforms, and the payload miniaturization have demonstrated being a true competitor of large spacecrafts for some applications. Table 3 summarizes the capabilities of CubeSat EO platforms (3U, 6U, and 27U). Nanosatellites are now becoming popular thanks to the CubeSat standard. Typical CubeSat missions can be implemented in 1 to 3 years, with typical budgets from 200 K to 1 M $ USD, including launch.

On the other side, ESA has promoted the development of a generic Small Geostationary Platform [14] (SmallGEO or SGEO) industrialized by OHB [15]. This flexible and modular platform has a lifetime of up to 15 years, a payload mass of up to 400 kg, and a payload power of up to 4 kW [16]. This platform was originally proposed to help European industries in the commercial telecom satellite market. However, the Earth Observation domain can also benefit from the capability of this platform in terms of available power and payload mass. In this way, an analysis of the EO technologies that are appropriate for use in small platforms is conducted in the next section.

**Table 2.** Summary of survey of commercial small platforms capabilities.

| Classification | Satellite Mass [kg] | Max. Payload Mass [kg] | Max. Payload Power (average) [W] | Max. Data Rate (Downlink) |
|---|---|---|---|---|
| Nano | $<10$ | $\leq 3$ [17] | $\leq 15$ [11,18] | $\leq 15$ Mbps [19] |
| Micro | 10–100 | $\leq 54$ [20] | $\leq 150$ [21] | $\leq 160$ Mbps [22] |
| Mini | 100–1000 | $\leq 600$ [9] | $\leq 1500$ [10] | $\leq 1.2$ Gbps [13] |

**Table 3.** Summary of survey of commercial CubeSat platforms capabilities.

| Classification | Approximate Size [cm] | Payload Mass [kg] | Payload Power [average/peak] [W] | Payload Data Rate [downlink] | References |
|---|---|---|---|---|---|
| 3U | $10 \times 10 \times 30$ | <3 | ≤15 | ≤15 Mbps | [17] |
| 6U | $10 \times 20 \times 30$ | <12 | ≤20 | ≤15 Mbps | [23] |
| 27U | $30 \times 30 \times 30$ | <50 | ≤90 | ≤100 Mbps | [20] |

## 3. Survey of Earth Observation Sensors and Measurements Requirements to Cover the Future Gaps on Copernicus

EO satellites have revolutionized the study of the environment, and are contributing to a more rational use of the natural resources, and environmental protection. The applications of the data supplied by these systems are enormous: disaster monitoring, weather forecast, maritime safety, marine resources monitoring, forestry, vegetation state, water cycle, energy budget, pollution control, water quality, climate change, and security; using radars, microwave and optical/IR radiometers, optical imagers or scanners. Table 4 presents the generic classification of the remote sensors. Instruments are classified in the following four categories: active or passive, either microwave or optical. Optical sensors measure the signals received around the visible part of the spectrum, from the Ultra-Violet (UV) to the Thermal Infrared (TIR). Microwave sensors use the signals in the microwave and millimetre-wave parts of the spectrum, typically from 1 GHz to 1 THz. Passive systems are based on the collection of the electromagnetic waves that are emitted/scattered by external sources, such as the Sun or other bodies. On the other hand, active systems such as radars and lidars, transmit an electromagnetic wave, either radio or laser, and measure the scattered/reflected signal from the Earth's surface or atmosphere. Microwave sensors do not rely on the Sun as source of illumination. These particular characteristics are especially important in Polar Regions that have extended dark periods in winter. In addition, microwaves are mostly unaffected by the cloud cover, except in some specific bands. This feature makes microwave sensors more suitable than optical sensors in these regions.

This section presents a survey of the selected EO technologies. In order to identify the potential EO sensors to improve the Copernicus space infrastructure, EO technologies are analyzed in depth based on the measurements with identified gaps, and the technological limitations. A total of 77 instruments have been surveyed, and their parameters (mass, power consumption, spatial resolution, swath, frequency bands, aperture, and orbit altitude) have been compiled from the Observing Systems Capability Analysis and Review (OSCAR) Tool [24], the Earth Observation Portal Directory [25], and companies websites (Appendix B). The best instruments in terms of data quality and suitable for the small platform are identified for each technology.

**Table 4.** Instrument categorization: potential instruments to complement the Copernicus system [6].

| | PASSIVE | | ACTIVE | |
|---|---|---|---|---|
| MICROWAVE | Radiometer | • Imager<br>• Sounder | Real Aperture Radar | • Altimeter<br>• Scatterometer |
| | Signals of Opportunity (SoOp) | • GNSS-R [a]<br>• Receiver of SoOP [b] | Synthetic Aperture Radar | • Altimeter<br>• Imager |
| | Receiver | • Automatic Identification System (AIS) | | |
| OPTICAL | Radiometer | • Multispectral<br>• Hyperspectral | Lidar | |
| | Sounder | | | |

[a] multi-static radar using satellite navigation signals of opportunity (SoOp). [b] e.g., Direct Broadcast Satellite (DBS) television at Ku-band or X-band.

### 3.1. Passive Microwave

#### 3.1.1. Microwave Imagers (MWIm)

The main applications of Microwave Imagers (MWIm) are atmospheric (X, K, Ka, and milimiter waves bands), oceanographic (C, X, K, and Ka bands), vegetation and soil moisture monitoring (P, L, S, C and X bands). High frequency microwave radiometers are particularly well suited for small platforms because of the antenna size constraints. These types of instruments can measure: wind speed [26,27], sea ice thickness [28,29], and sea ice cover [30], among other variables. Table A4 presents the features of some microwave radiometers, in terms of frequency bands, spatial resolution, antenna size, swath, mass, power consumption, and data rate. Assuming only one payload per platform, the affordable platforms (nano, micro, mini, and large) for the instruments are identified according to the power and mass requirements. This information is valuable in order to choose the potential instruments that will complement the Copernicus Space segment, trying to make them compatible with the smallest possible platforms, while fulfilling the user requirements. The measurement gaps that can be covered with this technology are: horizontal wind speed over the sea surface (MWIm with channels around 7, 10, 19, 37 GHz or 19 and 37 GHz), sea ice monitoring (cover, type, drift, MWIm with channels around 7, 10, 19, 37, and 90 GHz), sea ice thickness (MWIm with channels around 1.4 GHz), soil moisture (MWI with channels around 1.4 GHz, or 7 GHz, or 11 GHz), and sea surface temperature (MWIm with channels around 7 and/or 10 GHz).

According to Table A4, two microwave imagers capable of measuring the variables with gaps have been identified. These are selected because they are suitable for small platforms and present good data quality, to cover the user requirements.

- A Tropical Rainfall Measuring Mission Microwave Imager (TMI) like instrument is capable of measuring wind speed (at 10.65, 19.35 and 37 GHz), sea ice cover (at 19.35, 37, and 85.5 GHz), and sea surface temperature (at 10.65 GHz). Modified versions of TMI for micro- or mini-platforms achieving a 10 km spatial resolution using an aperture size (inflatable antenna) of 3.4 m @ 10.65 GHz from 600 km height will suit LEO polar Sun-Synchronous Orbit (SSO, ∼14 orbits/day) reducing the revisit time to 3 h in the Polar Regions. The required number of satellites was optimized in [31].
- The available L-Band microwave sensors, such as Microwave Imaging Radiometer using Aperture Synthesis (MIRAS) and Soil Moisture Active-Passive (SMAP) are suitable for mini-platforms. L-band microwave radiometers are capable of measuring the variables with the detected gaps, such as sea ice thickness and soil moisture. Sea ice thickness presents gaps in the revisit and latency times. The revisit time required is 24 h, and a latency time of 1 h. Surface soil moisture monitoring presents gaps in the accuracy 0.01 $m^3/m^3$ and the latency time 1 h.

#### 3.1.2. Microwave Sounders (MWS)

In the last few years, intensive work has been conducted to develop missions to prove the feasibility of using microwave sounders on nano-platforms, such as MicroMas [32], and the Earth Observing Nanosatellite-Microwave (EON-MW) [33]. The measurement with gaps that can be analyzed with this technology is the atmospheric pressure over the sea surface.

Table A5 presents a survey of the representative current and future missions with microwave sounders capable of measuring the atmospheric pressure over the sea surface. The gaps for this variable are the revisit and the latency times. To fill these gaps, a constellation of microwave sounders based on CubeSats missions could observe fast weather phenomena requiring high revisit time (3 h or less). A good example of CubeSat mission is EON-MW. The payload is a dual-reflector radiometer with a mass of 4 kg, an antenna size of 11 cm, and spatial resolution of 30 km on altitude of 600 km at 54 GHz.

### 3.1.3. Signals of Opportunity (SoOp): GNSS-R, and Receiver of SoOp

The utmost sensors used for oceanography (SARs and radar altimeters) have features that make them difficult to board on nano-satellites, most notably the power requirements, and the antenna size. An attractive option to explore the sea surface topography is the use of reflected Global Navigation Satellite Systems (GNSS) signals [34,35]. GNSS reflectometry is a favourable technique to perform some ocean measurements with small satellites [36]. The advantage of this technique is the capability to operate in all-weather conditions with a spatial resolution of ∼25 km. In the last two decades, a big effort has been made to develop models that prove the feasibility of using GNSS signals, proving to be successful for sea surface, altimetry measurements [37,38], wind speed [39,40], soil moisture [41–45], ice thickness [46], ice cover [47], and others. A few characteristics of GNSS-R missions have been identified and summarized in Table A6.

The current and planned missions using GNSS-R technology are presented in Table A6, such as TechDemosat-1 (TDS-1) [48], the Cyclone Global Navigation Satellite System (CYGNSS) [36], and FSSCAT [49,50].

TDS-1 was launched in June 2014 and it includes a GNSS-R payload with a mass of around 1.5 kg and approximately 10 W power consumption . It demonstrated the capabilities of GNSS-R for low power, low cost, and low mass. This payload measures complete delay-Doppler Maps (DDM) providing scientific-quality data [51]. The CYGNSS mission takes advantage of a constellation of eight microsatellites (weighting 17.6 kg) that provide nearly gap-free Earth coverage over Equatorial regions, with an average revisit time of seven hours and a median revisit time of three hours. CYGNSS was launched on December 2016. FFSCAT is a tandem mission of two 6U Cubesats ($^3$Cat-5/A and $^3$Cat-5/B) featuring a hybrid microwave radiometer/GNSS- Reflectometer and a hyperspectral imager. FSSCAT will be the first nanosatellite mission to complement the Copernicus program [49]. Its main focus is over Polar Regions, and it will be launched in 2019.

The European Space Agency (ESA) conducted the studies of a space-borne demonstrator called Passive Reflectometry and Interferometry System In-Orbit Demonstrator (PARIS IoD) [52–54]. PARIS IoD was later reincarnated into the GEROS experiment on board the International Space Station [55], but it was never implemented.

Novel techniques using signals of opportunity, such as from Direct Broadcast Satellite (DBS) television at Ku- or X-bands, can be used to measure precipitation and winds over the sea surface [56], and these signals are sensitive to detect fluctuations of the sea surface roughness.

In this regard, the SGR-ReSI [57] payload onboard TDS-1 is selected as a possible candidate to cover the measurements with gaps such as wind speed over the sea surface (horizontal), sea ice cover, sea ice thickness, and soil moisture [6].

### 3.1.4. Receiver: Automatic Identification System (AIS)

Although not an EO technique, Automatic identification systems (AIS) could also be a potential technology for emergency and management for the Copernicus services. AIS is an automatic tracking system used by ships and vessel traffic services. The AIS is a standardized receiver using two channels in the maritime VHF band. It has a positioning system with electronic navigation sensors such as a gyrocompass or rate of turn indicator. The main advantages of this system are the accuracy of the position, course, and speed information. Additionally, the International Maritime Organization (IMO) has normative guidelines to put AIS on board for all passenger ships larger than 300 GT. Additionally, the latency can be reduced thanks to an update rate of ∼3 min. In addition, it is suitable for nano-satellites [58] (low size, low power, low weight, and these can be translated into low system cost) (Table A7).

### 3.2. Passive Optical

This type of technology has shown its feasibility for small missions [59,60]. For example, for an optical instrument in the visible part of the spectrum, with a ground resolution better than 10 m, and an aperture of 10 cm (CubeSat size), the altitude of the satellite should be less than 500 km.

The data provided by passive optical instruments, from the ultraviolet to the far-infrared wavelengths can be used for weather forecast, vegetation, atmosphere, ocean and land studies. The main limitation of optical sensors is that data cannot be acquired in night-time (visible and near infrared parts of the spectrum) or cloudy conditions, and cloudy weather is very frequent in Polar Regions.

In this manuscript, the classification of optical sensors as radiometer imager and atmospheric sounders, and its subclassification between multispectral and hyperspectral is studied. Radiometer imagers measure the intensity of electromagnetic radiation in the visible or infrared bands, and sounders measure the vertical distribution of atmospheric parameters such as pressure, temperature, and humidity. Multispectral instrument refers to a maximum number of tens of bands, and hyperspectral radiometers consist of hundreds of narrow and continuously distributed bands (10–20 nm).

#### 3.2.1. Radiometer: Multispectral and Hyperspectral

Table A8 presents the features of the available multispectral and hyperspectral radiometers instruments, in terms of wavelength, spatial resolution, aperture size, swath, mass, power consumption, and data rate. The variables of interest that can be measured with optical sensors for the Marine for Weather Forecast, Sea Ice Monitoring, Fishing Pressure, and Agriculture and Forestry: Hydric stress use cases are the Sea Surface Temperature (SST), atmospheric pressure over the sea surface, ocean chlorophyll concentration, ocean imagery and weather leaving radiance, Color Dissolved Organic Matter (CDOM), detection of water in crops, estimation of crop evapotranspiration and the sea ice cover.

A good example of multispectral radiometer on micro-platform is AVHRR/3 [61] and also has good performance, and it could support the measurements with detected gaps, such as SST, ocean chlorophyll concentration, ocean imagery and weather leaving radiance, CDOM, detection of water in crops, estimation of crop evapotranspiration, sea ice cover, and atmospheric pressure over the sea surface (it can be inferred through measurements in the infrared band).

#### 3.2.2. Sounder: Multispectral and Hyperspectral

A good example of hyperspectral infrared sounder capable of measuring atmospheric pressure over the sea surface on CubeSat is EON-IR [62]. This instrument is under development with spatial resolution comparable to legacy sounders such as Infrared Atmospheric Sounding Interferometer (IASI), Atmospheric Infra-Red Sounder (AIRS), and Cross-track Infrared Sounder (CrIS).

Table A9 presents the details of the available multispectral and hyperspectral sounders instruments, in terms of spatial resolution, aperture size, swath, mass, power consumption, and data rate. For each optical sensor, it classifies (nano-, micro-, mini-, and large-satellite) according to the payload power and mass that can support the available commercial platforms summarized in Table 2.

### 3.3. Active Microwave

Several missions have been launched with active microwave instruments that can be grouped into three main families: Scatterometers, Synthetic Aperture Radars (SAR), and Radar Altimeters (RA). This section describes the variables of interest that can be measured with satellite-based active microwave sensors: wind speed, and direction over the sea surface using radar scatterometers, SAR and SAR altimeters; sea level, significant wave height, wave and wind speed using RA; and dominant wave direction, significant wave height and sea ice cover by SAR. Then, each variable is presented with the available active microwave technology, and the new trends of these sensors in small satellites.

#### 3.3.1. Real Aperture Radar Altimeter

Radar altimeters measure the distance of the Earth's surface underneath the spacecraft by measuring the time between transmitting the signal and receiving the echo. Microwave radar altimeters have been used for a wide range of applications that can be grouped as: (a) geodesy and geophysics, study the Earth's shape and size, on the ground as well as on the sea surface [63]; (b) ocean applications (ocean surface currents, wind speed, significant wave height); (c) ice sheets and sea ice (sea ice thickness, and glacier topography) [64]; (d) climate (ocean topography and the heat exchange with the atmosphere); and (e) hydrology.

Nowadays, altimeter constellations on small platforms are deemed important, since they bring improved temporal resolution, and some ocean phenomena can only be perceived if subject to an almost continuous observation. At the same time, a shorter revisit time represents an increase in the spatial coverage and a finer spatial sampling grid. Equally, SSO should be avoided because of the errors associated with solar tidal effects.

Examples of recent altimetry missions are presented in Table A10. Typical requirements are: 100 W average power consumption, 1.2 m antenna diameter, 61 kg payload mass. The implementation on nano- platforms for radar altimeters may partially degrade the quality of the measurements. Additionally, nadir looking altimeters do not provide a wide swath. In this way, constellations of small satellites embarking a compact nadir altimeter [65] could improve the temporal/spatial sampling and therefore closing the gap with current planned missions.

#### 3.3.2. Real Aperture Radar Scatterometers

Current and planned scatterometers missions have been identified and are summarized in Table A11. Earth Observation missions based on scatterometers typically operate at C-, and Ku-bands, and present spatial resolutions from 10 to 50 km. Current and future contributing missions to the Copernicus system with radar scatterometer are: ASCAT and SCA, ASCAT/Metop-A/B/C (2007 to 2021), with global coverage every 1.5 days and 12.5 km spatial resolution for basic sampling, SCA/Metop-SG-B1/B2/B3 (from 2022 to 2030) with near global coverage every 1.5 days, from 15 to 20 km of spatial resolution with sampling at 6.25 km intervals.

The main variables derived from radar scatterometer data are wind speed and vector over sea surface [66], but scatterometers are also capable to obtain surface soil moisture indices [67], leaf area index [68], snow water equivalent, snow cover [69], and sea ice extent measurements [70] Table A11 shows the characteristics of the radar scatterometer. The power consumption of these sensors is in the range of 210–540 W, and mass is in the range from 260 to 600 kg. According to the requirements of power consumption, size and mass, this payload can be carried over mini- or large-satellites.

#### 3.3.3. Synthetic Aperture Radar (SAR) Altimeter

SAR altimeter differs from real aperture radar altimeter (conventional) in that it exploits coherent processing of groups of transmitted pulses, while conventional altimeters is exploited to make the most efficient use of the power reflected from the surface. The SAR altimeter offers many potential improvements over conventional altimetry for measurements, since it increases the resolution and offers multilook processing.

Currently, three mini-satellites are dedicated to altimetry with SAR processing, such as SARAL, Sentinel-3A, and Sentinel-3B. The planned missions are Sentinel 6 (Jason-CS). Table A12 summarizes the main characteristics of radar altimeters with SAR processing. Typical requirements are similar to the conventional altimeters for mini-platform: 100 W average power consumption, 1.2 m antenna diameter, 63 kg payload mass.

The geophysical variables of interest to analyze with SAR altimeter are ocean surface currents, significant wave height, dominant wave direction, sea ice cover, sea ice type, sea ice thickness, and horizontal wind speed over the sea surface.

3.3.4. Synthetic Aperture Radar (SAR) Imager

Spaceborne SAR imager sensors have been widely used for ocean monitoring (e.g., sea-ice cover, oil spills monitoring, sea-ice type, wave direction, dominant wave period, sea level, etc.), and land applications (e.g., soil moisture indices, vegetation monitoring, classification, fire fractional cover, fraction of vegetation over land, landslides and motion risk assessment, permafrost, and others) to support the environment management, with resolutions comparable to those of optical systems. The manufacturing and implementation related to a small SAR satellite mission have opened a market for a new technology which has recently been developed: the constellations of small SAR satellites, being the principle of Fractionated and Federated Satellites (FSS) [71], and/or bistatic SARs as companion satellites (e.g., SAOCOM [72]).

The use of SARs imager in small satellites poses some major challenges, such as the antenna dimensions and power requirements of the system. Another challenge is how to generate the power required by this sensor, reducing the transmitted power, resulting in a narrow swath and therefore increasing the revisit time. In this line, SARs are now feasible in small platforms—for example, NovaSAR-S [73] and ICEYE's Synthetic Aperture Radar [74]. NovaSAR-S is a novel platform for small synthetic aperture Radar (S-band) development by Surrey Satellite Technology Ltd. (Guildford, United Kingdom), with a mass of 500 kg and peak power of 1.8 kW. The antenna is a microstrip patch phased array with size of 3 × 1 m. ICEYE's Synthetic Aperture Radar is a microsatellite developed by ICEYE, with a satellite mass of 100 kg, and phase array antenna at X-band. According to the frequency band of the SAR, beyond 2028, there will be no X-band SAR mission in orbit, but there will be L- and C-band SARs mission (Figure 2). On this subject, the frequency band selected for SAR instrument is X-band, in order to obtain a smaller instrument and cover the frequency gap.

The geophysical variables of interest to analyze with SAR imager are iceberg tracking, sea ice cover, sea ice type, sea ice thickness, sea ice drift, sea ice extent, wind speed, ocean surface currents, dominant wave direction, dominant wave period, wind speed, and significant wave height. Nevertheless, single, large SAR satellites are not compatible with the requirements of 3 h of revisit time. Constellations of small SAR Satellites are under development or implementation stages [74]. In contrast, large SAR Satellites have been in orbit for years. Small SAR satellites can replace large SAR, for some specific applications requiring medium resolution imagery and smaller areas covered (due to power limitations). If the frequency band is higher (X-band), the spatial resolution and swath wide can be adjusted, therefore reducing the size and mass of the system. Table A13 presents a survey of the representative SAR image missions and classifies each instrument into mini or large according to capabilities of commercial platforms surveyed in the previous chapter.

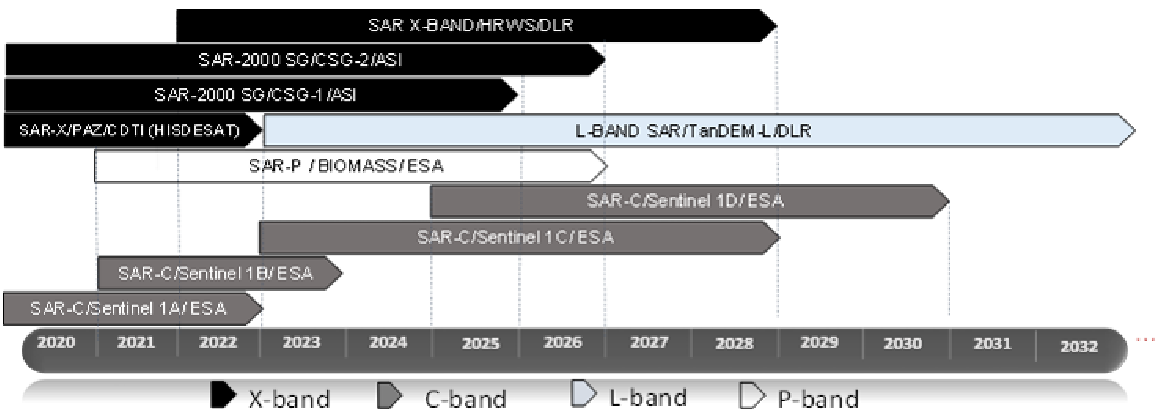


**Figure 2.** Frequency bands of future (2020–2030) European Union (EU) mission carrying Synthetic Aperture Radar (SAR) imager instruments.

### 3.4. Active Optical

Lidar

Active Optical Instruments or Lidars use pulsed laser emissions to measure atmospheric profiles and Earth surface applications such as vegetation height. Due to the short wavelengths, the laser pulse propagation through the atmosphere is scattered and attenuated by air molecules and aerosols. On the Earth's surface, the vegetation and canopy also cause scattering. A small portion of the scattered light is sent back to the instrument which collects, and detects it. Subsequently, the electric signal is digitized through a Lidar signal numerical processing. Over the ocean, the variables that can be measured with Lidars are sea ice thickness, sea level and ocean dynamic topography.

Lidars can be divided into two broad categories: (i) atmospheric profilers producing also the total column content for atmospheric composition, i.e., particles layers and key trace gases, and (ii) altimeters with decimeter to meter accuracy for topography retrieval and canopy vertical distribution. The objectives of relevant Lidars are:

- Surface topography, ice sheet [75], and canopy [76] (e.g., ICESat-1).
- Climate and Radiation Budget by profiling clouds and aerosols optical and microphysical properties (e.g., NASA CALIPSO since 2006 [77], and ESA/JAXA EarthCARE [78], to be launched in 2021).
- Atmospheric dynamics or horizontal winds, (e.g., ESA Atmospheric Dynamic Mission ADM-Aeolus [79] was launched on 22 August 2018). Lidar instruments present the following main characteristics:
- Operating wavelengths in the UV, VIS, NIR, and SWIR; possible dual-wavelength, polarimetry, and two receivers (for Mie and Rayleigh scattering).
- Spatial resolution in the range of 100 m to a few tens of centimeters for LIDAR altimeters.
- Non-scanning, either nadir-viewing or oblique.

Doppler LIDARs generally operate in the UV to track aerosol and air molecules and it are used for track aerosol and air molecules. Backscatter LIDARs are typically operated at one or two wavelengths (UV or VIS + NIR), often with amount of polarizations cross-talk into a succession of atmospheric backscatter measurements (rotatable half-wave plate) to discriminate between spherical and non spherical particles in the atmosphere, the nadir view brings the capability to measure aerosol profiles, cloud top height and atmospheric discontinuities, and the multi-beam to perform a large swath. Lidars altimeter operated at two wavelengths (VIS + NIR) can measure with very high vertical resolution and horizontal resolution (for sea-ice elevation, and ice boundaries). Differential absorption LIDARs (DIAL) operate at one wavelength centered on the absorption peak of one trace gas (e.g., $O_3$, $H_2O$ and $CO_2$). The main limitation of this technology is the narrow swath. The variable with a gap that can be analyzed with Lidar is the sea ice thickness.

Table 5 summarizes all technologies discussed in this section: radiometer imager, radiometer sounder, GNSS-R, AIS, scatterometers, altimeters, altimeter with SAR processing, SARs imager, Passive optical and Lidars. The measurements with gaps that can be measured for each technology are identified. The studied technologies are feasible on small platforms taking into account the survey of the commercial platform addressed in the previous section. Now, the best technology option needs to be analyzed, based on the future observations required by the Copernicus space infrastructure.

**Table 5.** Mapping of the potential technologies to cover measurements with gaps.

| Technology Type | | | Measurements |
|---|---|---|---|
| Microwave | Passive | Radiometer Imager (X-, K-, Ka-, W-bands) | Wind speed over sea surface (horizontal) [b]<br>Sea ice cover [b]<br>Sea ice type [a]<br>Sea ice drift [a]<br>Sea surface temperature [a] |
| | | Radiometer Imager (L-band) | Soil moisture at the surface [c]<br>Sea ice cover [b]<br>Sea ice thickness [a]<br>Crop growth & condition |
| | | Radiometer Sounder (50–60 GHz) | Atmospheric pressure (over sea surface) [c] |
| | | Signals Oportunity: GNSS-R | Soil moisture [b]<br>Sea ice thickness [a]<br>Dominant wave direction [b]<br>Wind speed over the sea surface (horizontal) [a]<br>Significant wave height [b]<br>Sea ice cover [b]<br>Ocean surface currents [b] |
| | | Signals Opportunity: Receiver of SoOp (X, Ku-band) | Wind speed over sea surface [a] |
| | | Receiver: Automatic Identification System (AIS) | Monitoring system: vessels [c] |
| | Active | Real Aperture Radar: Altimeter | Ocean surface currents [c]<br>Significant wave height [b]<br>Dominant wave direction [b]<br>Sea ice thickness [a]<br>Wind speed over sea surface (horizontal) [a] |
| | | Real Aperture Radar: Scatterometer | Wind speed over sea surface (horizontal) [c]<br>Sea ice extent [a]<br>Sea ice cover [a] |
| | | Synthetic Aperture Radar (SAR): Altimeter | Ocean surface currents [c]<br>Significant wave height [b]<br>Dominant wave direction [b]<br>Sea ice type [b]<br>Sea ice cover [b]<br>Sea ice thickness [a]<br>Wind speed over sea surface (horizontal) [a] |
| | | Synthetic Aperture Radar (SAR): Imager | Ocean surface currents [c]<br>Iceberg tracking [c]<br>Sea ice drift [c]<br>Sea ice extent [c]<br>Sea ice type [c]<br>Sea ice cover [c]<br>Dominant wave direction [b]<br>Dominant wave period [b]<br>Significant wave height [b]<br>Sea ice thickness [a]<br>Wind speed over sea surface [a]<br>Ocean imagery and water leaving radiance |
| Optical | Passive | Multispectral radiometer (VIS/NIR/TIR) | Ocean chlorophyll concentration [c] ($\lambda$: 442.5, 490, 510, 560 nm)<br>Ocean imagery and water leaving radiance [c] ($\lambda$: 485, 560, 660, 2100 nm)<br>Color Dissolved Organic Matter (CDOM) [c] ($\lambda$: 442.5, 490, 510, 560, 665 nm)<br>Sea surface temperature [c] ($\lambda$: 3.7, 4.05, 8.55, 11, 12 μm)<br>Sea ice cover [a] ($\lambda$: 640, 1610 nm)<br>Detection of water stress in crops [c]<br>Estimation of crop evapotranspiration [c] |
| | | Hyperspectral radiometer (VIS/NIR) | CDOM [c]<br>Sea ice cover [b] |
| | | Sounder (IR) | Atmospheric pressure over sea surface [c]<br>Sea surface temperature [c] |
| | Active | Lidar | Sea ice thickness [b] |

The data relevance of the instrument depends on its ability and limitations to obtain the measurements: [a] Marginal relevance; [b] medium relevance; [c] high relevance.

## 4. Potential Instrument, Suitable Platforms, and Technological Limitations

After the survey of the suitable EO technologies in terms of the spatial resolution, swath, mass and power consumption, in this section, the suitable small commercial platforms and technological limitations of the potential sensors are identified. Tables 6 and 7 show the potential technologies studied in this work, with the suitable platforms and limitations with respect to the needs detected in the horizon 2020–2030. Platforms are selected according to their capacity to support the instrument mass and power consumption (available commercial platforms surveyed, Tables A1–A3). Additionally, it takes in to account the platforms with minor categorization (e.g., nano-, micro-, or mini-platforms), that satisfy both requirements. Special attention has been paid to the possibility to use new techniques and smaller platforms, focusing on the quality of the measurements as compared to the ones generated by full-fledged payloads onboard large spacecrafts. Indeed, since a small platform also means less volume, mass, power and data rate for the payload, the measurements are usually of reduced quality. Depending on the mission (i.e., environmental data), this may be compensated by more frequent data acquisitions (exchange between measurement quality and revisit time), yet to be evaluated on a case-by-case basis. A brief the potential instruments, suitable platforms, and technological limitations are explained below:

- GNSS-R (1.4 kg, 12 W) instruments are suitable for nanosatellites (3U or 6U). Table 6 presents sample available commercial platforms for the SGR-ReSi [57], such as the Endeavour-3U [18] and the MAI-3000 [17]. Endeavour by Tyvak Nanosatellite Technology Inc. (San Luis Obispo, CA. United States of America), is a 3U platform with 15 W of average payload power, 3 deg of pointing control. MAI-3000 by Maryland Aerospace, is a 3U platform with 12 W of payload power and 3 kg of available payload mass. The main limitation of GNSS-R altimetry data is the poorer (decimetric) resolution and accuracy ($\sim$20 cm for SSH, and 2 m/s for wind speed) are offset by the much larger number of simultaneous observations from different specular reflection points [80].
- Another good example are microwave sounders on small-platforms such as EON-MW [33], for measuring the atmospheric pressure over the sea surface. However, the antenna system must be redesigned to achieve the spatial resolution required. For a 10 km spatial resolution, at 50 GHz, the require antenna aperture is 36 cm, from an altitude of 600 km. Table 6 summarizes a list of the available commercial micro-platforms suitable for this instrument.
- Microwave imagers at X-, K-, Ka-, and W- bands are particularly well suited for implementation on small platforms (Table 6). TMI is a light instrument suitable for mini-satellites, with X-, K-, Ka-, and W- bands capable of measuring and covering the gaps for wind speed, sea ice cover, sea ice type, and sea surface temperature variables. For sea surface temperature, microwave radiometers improve the coverage in polar regions because of their all weather capabilities. In order to obtain a spatial resolution of 10 km at 18.7 GHz from 600 km height, a 2.2 m antenna is required. On the other hand, an SSM/I type of instrument with a modified antenna, could be implemented in a micro-platform in order to cover wind speed over the sea surface, sea ice cover, and sea ice measurements, with the required performance. L-band radiometers contribute to sea ice thickness monitoring, agriculture (soil moisture) and forestry measurements. Those instruments are suitable for mini-platforms (Table 6). The main limitation is their coarse resolution. Inflatable antennas must be used to reduce the footprint size, or aperture synthesis techniques could be implemented [81]. ELiTeBUS 1000 [10] by Thales Alenia Space (Cannes, France) is an available commercial small-platform suitable for this instrument. ELiTeBUS 1000 is a platform for Medium Earth Orbit (MEO) and Low Earth Orbit (LEO) orbit with 1000 to 1500 W of available payload power.
- Scatterometers contribute to the Marine for Weather Forecast and Sea Ice Monitoring use cases. The instrument taken as a reference is the SCAT on board the CFOSAT mission [25,82], the power consumption of this sensor is less than 200 W, and the mass less than 200 kg. According to the power consumption and mass requirements, this payload can be carried on board mini-platforms

(Table 7). Scatterometers are valuable sensors for wind measurements. However, the main limitations are the coarse accuracy and spatial resolution of the data. However, their wide swath and the possibility of scatterometer constellations open the door to improve the accuracy and spatial resolution, combining the data from multiple passes of different satellites.

- For radar altimeters, the accuracy of the measurements depends on the Pulse Repetition Frequency (PRF), which is directly driven by the power available on-board to the payload. Since the power available on-board decreases with solar panel size, the accuracy of the measurements on a small satellite is also expected to be degraded as compared to that of large satellites. For example, if the power consumption is reduced by a factor of 4, the PRF is reduced roughly by the same factor, and the Root-Mean-Square (RMS) error increases by a factor of 2. For the Jason-2 altimeter (power consumption ∼70 W), a reduction of its power consumption to 1 W, would increase the sensor error level from 2 cm to ∼16.7 cm, which is actually comparable to GNSS-R [55,82]. It is easy to understand that the types of products that can be generated with this accuracy are different from the ones generated with an SRAL radar altimeter, but one must also consider that the number of radar altimeters with a transmitted power of 1 W that can be manufactured and launched at the same cost as for a high accuracy radar altimeter is much larger. These few examples illustrate the fact that the quality and frequency of the measurements have to be considered in the overall comparison process. In some cases, the concept of operations may partially be compensated by the degradation of the quality of the individual measurements (e.g., part-time measurement instead of systematic measurement if the power available on board is the main parameter driving the performance of the measurement).
- SAR sensors are one of the most effective instruments for ocean, land, and ice observation. A good example of miniaturization of this technology is the Severjamin-M instrument (Meteor-M N missions) [83], an X-band SAR with power consumption of 1 kW and a mass of 150 kg, including the mass of the antenna of 40 kg. The main technological limitation is the narrow swath, but this could be compensated with a constellation of SAR satellites.
- Optical payloads are characterized in terms of image quality such as the Ground Sampling Distance (GSD), the Modulation Transfer Function (MTF), and the Signal-to-Noise Ratio (SNR). To be able to interpret an image (e.g., in the maritime surveillance, the capability to estimate the type of a boat), the GSD is not sufficient, since a degraded MTF (i.e., blurred image) or a degraded SNR (noisier image) would prevent it. Ensuring a good MTF and SNR for a given GSD requires a minimum aperture for the optical instrument, and reducing it below this minimum value will limit the type of applications. Image quality is also limited by the platform's attitude control system, i.e, any jitter in the pointing will blur the image. This has also to be taken into account as smaller platforms exhibit poorer performances.

**Table 6.** Mapping of potential passive sensors and platforms to meet the user requirements.

| Technology Type | Measurements | Instrument Limitations | Instruments Identified | |
|---|---|---|---|---|
| Microwave Radiometer Imager<br>(X-, K-, Ka-, W-bands) or<br>(K-, Ka-, W-bands) | Wind speed over sea surface<br>Sea ice cover<br>Sea ice type<br>Sea ice drift<br>Sea surface temperature (at X-band) | Coarse spatial resolution and accuracy | TMI [25] | SSM/I [84] |
| | | | **Available commercial platform (Non-exclusive)** | |
| | | | NAUTILUS<br>(NEMO-150) [85]<br>SSTL-150 ESPA [86]<br>BCP-100 [87]<br>TET-XL [13] | SN-50 [21]<br>Altair [20] |
| Microwave Radiometer Imager<br>(L-band) | Surface soil moisture<br>Sea ice cover<br>Crop growth & condition<br>Sea ice thickness | Coarse spatial resolution | MIRAS [25,88] | SMAP [25,89] Aquarius [25] |
| | | | **Available commercial platform (Non-exclusive)** | |
| | Sea ice thickness | Accuracy | ELiTeBUS 1000 [10]<br>LEOStart-2 BUS [90] | |
| Microwave Radiometer sounder<br>(50-60 GHz) | Atmospheric pressure<br>(over sea surface) | Coarse spatial resolution | ATMS [25] | Miniature microwave sounder EON-MW [33] |
| | | | **Available commercial platform (Non-exclusive)** | |
| | | | SSTL-300/-600 [92,93]<br>SN-200 [94]<br>Eagle [90]<br>TET-XL [13] | NEMO / DEFIANT [85]<br>SSTL-12/-X50/-100 [22,91,92]<br>SMALL SAT 27U [12]<br>SN-50 [21]<br>Altair [20]<br>LEOS-30 [95]<br>BCP-50 [96] |
| Signals of Opportunity (SoOp): GNSS-R | Surface soil moisture<br>Ocean surface currents<br>Sea ice thickness<br>Significant wave height<br>Wind speed over sea surface | Accuracy | SGR-ReSI [57] | GEROS-ISS [80] |
| | Dominant wave direction<br>Surface soil moisture | Coarse spatial resolution | **Available commercial platform (Non-exclusive)** | |
| | Sea ice cover | No specific limitation | Endeavour-3U [18]<br>MAI-3000 [17] | ELiTeBUS 1000 [10]<br>LEOStart-2 BUS [90] |

**Table 6.** *Cont.*

| Technology Type | Measurements | Instrument Limitations | Instruments Identified | |
|---|---|---|---|---|
| Receiver: AIS | Monitoring system vessels | No specify limitation | SD AIS Receiver [58] | NAIS [97] |
| | | | **Available commercial platform (Non-exclusive)** | |
| | | | GOMX 2U/3U [98]<br>THUNDER (3U), GRYPHON (GNB) [85]<br>Endeavour-3U [18]<br>MAI-3000 [17]<br>SMALL SAT 6U [12] | GOMX 3U [98]<br>SMALL SAT 6U [12]<br>MAI-3000 [17]<br>Endeavour-3U [18] |
| Multispectral radiometer (VIS/MWIR/TIR) | Ocean chlorophyll concentration<br>Ocean imagery and water leavin radiance<br>CDOM<br>Sea surface temperature<br>Sea ice cover | Cloud sensitivity<br>Day light only | AVHRR/3 [25] | VIRS [25] |
| | | | **Available commercial platform (Non-exclusive)** | |
| | Detection of water stress in crops<br>Estimation of crop evapotranspiration | Coarse spatial resolution<br>Cloud sensitivity<br>Day light only | SSTL-12 [22]<br>SSTL-X50 [91]<br>SN-50 [21]<br>Altair [20] | SN-50 [21]<br>Altair [20] |
| Hyperspectral radiometer (VIS/NIR) | Sea ice cover<br>CDOM | Cloud sensitivity<br>Day light only | CHRIS [25] | COMIS [25] |
| | | | **Available commercial platform (Non-exclusive)** | |
| | | | LEOS-50/-100 [95]<br>Small sat 12 U and 27U [12]<br>SSTL-12/-X50/-100 [22,91,92]<br>BCP-50 [96]<br>Altair [20]<br>SN-50 [21] | MAI-6000 [23]<br>NEMO [85]<br>LEOS-30 [95]<br>DEFIANT [85]<br>SMALL SAT 12U [12] |
| Hyperspectral sounder (IR) | Atmospheric pressure (over sea surface)<br>Sea surface temperature | Cloud sensitivity | EON-IR[25] | CrIS [25] |
| | | | **Available commercial platform (Non-exclusive)** | |
| | | | MAI-6000 [23]<br>NEMO, DEFIANT [85]<br>LEOS-30/-50/-100 [95]<br>SN-50 [21]<br>Altair [20]<br>SMALL SAT 16U [12]<br>SSTL-X50/-100 [91,92]<br>BCP-50 [96] | DAUNTLESS [85]<br>SN-200 [94]<br>Eagle-1M, LEOStart-2 BUS [90]<br>LEOSTART-500XO [9]<br>SSTL-600 [92]<br>ELiTeBUS 1000 [10] |

The background color in the Table indicates the platform suitable for the instrument according to the power and mass requirements: very lightgray: nano-platform; light gray: micro-platform; gray:mini-platform.

**Table 7.** Mapping of potential active sensors and platforms to meet the user requirements.

| Technology Type | Measurements | Instrument Limitations | Instruments Identified | |
|---|---|---|---|---|
| Real Aperture Radar scatterometer | Wind speed over sea surface (horizontal)<br>Sea ice extent<br>Sea ice cover | Accuracy | RapidScat [24] | SCAT [25,82] |
| | | | **Available commercial platform (Non-exclusive)** | |
| | | | SSTL-600 [92]<br>LEOSTART-500XO [9]<br>LEOStar-2 BUS [90]<br>EliTeBUS 1000 [10] | DAUNTLESS [85]<br>BCP-100 [87]<br>SN-200 [94]<br>Eagle-1M [90]<br>SSTL-600 [92]<br>LEOSTART-500XO [9]<br>LEOStar-2 BUS [90]<br>EliTeBUS 1000 [10] |
| Real Aperture Radar Altimeter<br><br>and/or<br><br>SAR Altimeter | Ocean surface currents<br>Significant wave height<br>Dominant wave direction<br>Wind speed over sea surface (horizontal)<br>Sea ice type<br>Sea ice cover<br>Sea ice thickness | Long-time analysis and narrow coverage | Altika [25] | SRAL [24], [25] |
| | | | **Available commercial platform (Non-exclusive)** | |
| | | | SN-50 [21]<br>Altair [20] | DAUNTLESS [85]<br>SSTL-150 ESPA/-300/-600 [86,92,93]<br>BCP-100 [87]<br>SN-200 [94]<br>Eagle-1M, LEOStar-2 BUS [90]<br>TET-XL [13]<br>LEOSTART-500XO [9]<br>ELiTeBUS 1000 [10] |
| SAR Imager | Ocean surface currents<br>Wind speed over sea surface<br>Dominant wave direction<br>Dominant wave period<br>Significant wave Height<br>Sea ice type<br>Sea ice cover<br>Sea ice thickness<br>Iceberg tracking<br>Sea ice drift<br>Sea ice extent<br>Ocean imagery and water leaving radiance | Narrow coverage | COSI [24] | Severjamin [25,83] |
| | | | **Available commercial platform (Non-exclusive)** | |
| | | | LEOStar-2 BUS [90] | LEOStar-2 BUS [90]<br>EliTeBUS 1000 [10] |
| Lidar Altimeter | Sea ice thickness | Cloud sensitivity<br>long time analysis<br>narrow covarage | ATLAS [24] | GEDI lidar [24] |
| | | | **Available commercial platform (Non-exclusive)** | |
| | | | ELiTeBUS 1000 [10]<br>LEOStart-2 BUS [90] | |

The background color in the Table indicates the platform suitable for the instrument according to the power and mass requirements: light gray: micro-platform; gray:mini-platform.

## 5. Reference Instrument Selection

The main requests of any satellite monitoring mission can be summarized as follows: (1) that observations are acquired with the required revisit time; (2) preferably in all weather conditions (clouds, rain, haze, and fog) and in all illumination conditions; (3) with a large swath to reduce the revisit time; (4) with the required radiometric and spatial resolutions; (5) with low manufacturing and launch costs, and with minimum deployment time in case of failure; and (6) keeping these parameters in mind, the reference instruments can be selected. In this way, the identification of instruments is based on the state-of-the-art at the payload level and the need to fulfill the gaps of the current Copernicus infrastructure.

Reference instruments and small platforms have been selected in the previous chapter. In this way, it has as strategy been implemented a significant reduction of the development time and cost, thanks to the adoption of commercial technologies, but it requires that these have a good performance of the measurement capabilities. In this regard, the capability of the instrument technologies is evaluated according to the trends in the design for small satellites. For each instrument, the mass and power consumption constraints, and data quality (spatial resolution, swath, and accuracy) are taken as a reference. This chapter evaluates if the instruments selected to meet the requirements (defined in [6]) in terms of spatial resolution and accuracy. Table 8 summarizes the performance requirements over each instrument:

- SGR-ReSI instrument presents a good performance for sea ice cover [99] because it satisfies the minimum requirement for spatial resolution and accuracy. For ocean surface currents, and significant wave height measurements satisfy the minimum requirement of spatial resolution at 25 km [100]. For other measurements, such as sea ice thickness [46], soil moisture [101], and wind speed [80] present worse performance than the minimum spatial resolution and accuracy requirements.
- EON-MW is a satellite project under development and presents an approximate performance that the Advanced Technology Microwave Sounder (ATMS) [33], in this way, it will be expected that the instrument satisfies the minimum requirements for accuracy of 5% and spatial resolution at 23 km for atmospheric pressure over sea surface measurements (channel from 50 to 60 GHz).
- MIRAS instrument presents a coarse spatial resolution $\sim$35 $\times$ 50 km for horizontal- and vertical-polarization. This instrument has an accuracy of 0.04 $m^3/m^3$ for soil moisture measurements [102] that is worse than 0.01 $m^3/m^3$ required. For sea ice thickness, the accuracy is worse than the 1 cm required [103], but it can have an accuracy of 5% for sea ice cover.
- SSM/I using an antenna (inflatable) of 2.2 m from 600 km orbit altitude can obtain a spatial resolution of 10 km and satisfy the minimal spatial resolution requirement for wind speed, and sea ice cover measurements. The accuracy for wind speed measurement can be until 1.5 m/s [104], and for sea ice data from 10% to 20% [105].
- TMI in order to meet the minimal spatial resolution requirement of 10 km (at 10.65 GHz) was proposed the modification of the aperture size of the antenna at 3.4 m (inflatable antenna). The accuracy for SST is of 0.5 K [104]. The accuracy is between 10% and 20% for sea ice data [105].
- AVHRR/3 presents a spatial resolution $\sim$1 km, and computes an accuracy better than 0.1 K [106].
- EON-IR is expected to be better than 0.25 K and present, with spatial resolution at 13.5 km.
- SCAT—the accuracy for wind speed monitoring is 2 m/s, and for sea ice monitoring is 5% .
- SRAL in SAR mode has a spatial resolution of 300 m, the accuracy for wind speed measurements is of 2 m/s [107]; for significant wave height, the accuracy is between 2 cm to 8 cm [108].
- Severjamin has a spatial resolution from 400 m to 1 km depending on the operation mode can satisfy many minimal requirements for some measurements.
- GLAS acquires the geophysical variables with a vertical spatial resolution of 10 cm, which does not satisfy the user requirement for sea ice thickness measurements.

**Table 8.** Reference instruments selected to cover the measurements with gaps.

| Instrument | Measurements | Requirements [109] | |
|---|---|---|---|
| | | Accuracy | Spatial Resolution |
| SGR-ReSI [57] | Soil Moisture at the surface | <0.01 m $^3$/m $^3$ | 10 km |
| | Sea ice thickness | 1 cm | 1 cm (vertical) |
| | Dominant wave direction | 10° | 1–15 km |
| | Wind speed over the sea surface | 0.5 m/s | 1–10 km |
| | Significant wave height | 0.1 m | 1–25 km |
| | Sea ice cover | 5 % | 12 km–10 m |
| | Ocean surface currents | 0.5 m/s 10° | 1–25 km |
| EON-Microwave [33] (Ka-, U-, D-bands) (22 channels) | Atmospheric pressure over sea surface | 5 % | 1–25 km |
| MIRAS [25,88] (L- band) | Soil Moisture at the surface | <0.01 m $^3$/m $^3$ | 10 km |
| | Sea ice thickness | 1 cm | 1 cm (vertical) |
| | Crop grow & condition | - | 2 km |
| | Sea ice cover | 5 % | 12 km–10 m |
| SSM/I [a] [84] (K, Ka, W) | Wind speed over sea surface | 0.5 m/s | 1–10 km |
| | Sea ice cover | 5 % | 12 km–10 m |
| | Sea ice type | 0.25/classes | 10 m |
| | Sea ice drift | 0.5 m/s 10° | 10 m |
| TMI [b] [24] (X, K, Ka, W) | Wind speed over sea surface | 0.5 m/s | 1–10 km |
| | Sea ice cover | 5 % | 12 km–10 m |
| | Sea ice type | 0.25/classes | 10 m |
| | Sea ice drift | 0.5 m/s 10° | 10 m |
| | Sea surface temperatture | 0.3 K | 1–10 km |
| AVHRR/3 [61] (VIS, NIR, MWIR, TIR) | Ocean chlorophyll concentration | 0.05 mg/m $^3$ | 1 km |
| | Ocean imagery and water leaving radiance | 5% | 1 km |
| | Color Dissolved Organic Mater (CDOM) | 5% | 1 km |
| | Sea Surface Temperature (SST) | 0.3 K | 1–10 km |
| | Detection of water stress in crops | 5% | 2–7 m |
| | Estimation of crop evapotranspiration | - | 1–10 m |
| | Sea Ice Cover | 5 % | 12 km–10 m |
| COMIS [24] (VIS, NIR) | CDOM | 5% | 1 km |
| | Sea Ice Cover | 5 % | 12 km–10 m |
| EON-IR | Sea Surface Temperature (SST) | 0.3 K | 1–10 km |
| | Atmospheric pressure over sea surface | 5 % | 1 km–25 km |
| SCAT [24] (Ku-band) | Wind speed over the sea surface | 0.5 m/s | 1–10 km |
| | Sea ice extent | 5% | 12 km–10 m |
| | Sea ice cover | 5 % | 12 km–10 m |

**Table 8.** *Cont.*

| Instrument | Measurements | Requirements [109] | |
|---|---|---|---|
| | | Accuracy | Spatial Resolution |
| SRAL[24,25] (C- & Ku-bands) | Ocean surface currents | 0.5 m/s 10° | 1–25 km |
| | Significant wave height | 0.1 m | 1–25 km |
| | Dominant wave direction | 10° | 1–15 km |
| | Sea ice type | 0.25/classes | 10 m |
| | Sea ice thickness | 1 cm | 1 cm (vertical) |
| | Sea ice cover | 5 % | 12 km–10 m |
| | Wind speed over the sea surface | 0.5 m/s | 1–10 km |
| Severjamin [25,83] (X-band) | Ocean surface currents | 0.5 m/s 10° | 1–25 km |
| | Iceberg tracking | 5% | 10 m |
| | Sea ice drift | 0.5 m/s 10° | 10 m |
| | Sea ice extent | 5% | 12 km–10 m |
| | Sea ice type | 0.25/classes | 10 m |
| | Sea ice cover | 5 % | 12 km–10 m |
| | Dominant wave direction | 10° | 1–15 km |
| | Significant wave height | 0.1 m | 1–25 km |
| | Sea ice thickness | 1 cm | 1 cm (vertical) |
| | Ocean Imagery and water leaving radiance | 5% | 1 km |
| | Wind speed over the sea surface | 0.5 m/s | 1–10 km |
| ATLAS [24] (VIS & NIR) | Sea ice thickness | 1 cm | 1 cm (vertical) |

[a] antenna size of 2.2 m. [b] antenna size 3.4 m. The background color in the requirements denotes: Green: Requirement met or is better; Yellow: Minimum requirement met; Red: Have worst performance that the minimum requirement. The background color in the instrument indicates the platform suitable according to the power and mass requirements: Very light gray: Nano-platform; Light gray: Micro-platform; Gray: Mini-Platform.

## 6. Quantitative Method to Identify the Potential Technologies to Cover the Future Copernicus Gaps

In order to identify the potential technologies to cover future gaps over Copernicus infrastructure, a quantitative method has been defined starting from the perspective of the instrument technologies and the variables with gaps. The analysis is centered on the list of the top 10 use cases and 20 variables detected with gaps, and the potential instruments which have been proposed in Table 8. A quantitative method has been applied to rank the technologies suitable to measure the variables with gaps, and identify which technologies cover most of the requirements. The rank order weights used is based on the user requirements, and measurements priorities.

A weighting system for the instrument performance parameter has been implemented. First, it defined the numerical score for each instrument capability based on user requirements (Table 9). Then, these numerical scores are evaluated for each measurement with gaps and each factor. In this way, the numerical score for latency is assigned for measurement that required latency time <1 h; for spatial resolution, a high score is assigned for measurement that required spatial resolution <1 km; for the revisit time, a high score for geophysical variables that required <3 h is assigned; for accuracy, a high score for measurements that require accuracy better than the state of the art is assigned. For payload mass and power consumption, the corresponding score for mini and micro platform is assigned; the measurement relevance was assigned taking the following:

- High relevance measurements: ocean surface currents, wind speed over sea surface, dominant wave direction, and significant wave height measurements.

- Medium relevance measurements: sea ice cover, sea ice type, sea surface temperature, and atmospheric pressure over the sea surface.
- Low relevance measurements: Ocean chlorophyll concentration, ocean imagery and weather leaving radiance, CDOM, monitoring system vessels, sea ice extent, sea ice thickness, iceberg tracking, sea ice drift, estimation of crop evapotranspiration, detection of water stress in crops, crop grow and conditions.

Then, the weights for each factor (latency, revisit time, spatial resolution, accuracy, payload mass, payload power, and measurement relevance) are derived by the normalization of the average of the numerical score assigned for each measurement:

$$W_j = \frac{\frac{1}{n}\sum_i^n Numerical_{score_i}}{\sum_j^m \frac{1}{n}\sum_i^n Numerical_{score_i}}, \tag{1}$$

where $i$ represents each measurement, and $j$ represents each factor. In order to identify the potential technologies, new numerical scores are assigned based on the instrument capabilities to measure the variables with gaps and how those meet the user requirements. Instrument attributes are defined in Table 10. The requirements for the geophysical variables are evaluated in terms of seven criteria (factors) or instrument capabilities:

- Latency is referred the time to be processed the data to obtain the product.
- Swath is related to the ability of the instrument in order to cover an area, a wide swath indicates minor revisit time.
- Spatial resolution is evaluated for the reference instruments according to the user requirements for each measurement.
- Accuracy is a component of the data quality; it is evaluated according to it being closed to the user requirements for each reference instrument.
- Payload mass is evaluated for each reference instrument, giving priority to the instruments that are best suited to smaller platforms.
- Payload power is related to the power consumption of the payload; it also brings priority to the instruments that are best suited to smaller platforms.
- Data relevance is the potential of the sensor to provide the measure based on sensing constraints (e.g., long time to analyze the data, data limited by cloud cover, and daylight only)

This scoring method assigns a lower score to the technologies that require a large instrument (large mass and high power consumption), and the technologies that present low data quality (low coverage, low spatial resolution, high latency, low accuracy, and low relevance for specific measurement). The score for each instrument is expressed in the following equation:

$$Instrument_{score-by-mensurement} = \sum_j^m \left(\frac{Numerical_{score}}{3} * W_j\right), \tag{2}$$

where $j$ represents each technology performances' parameters such as latency, spatial resolution, swath, accuracy, payload mass, payload power consumption, and data relevance for each potential instrument; $Numerical_{score}$ is assigned to each instrument by measurement (0, 1, 2 or 3); and $W_k$, is the weight assigned for each factor obtained of Equation (1) (Table 9, second column).

Four critical use cases were evaluated, such as Marine for Weather forecast, Sea Ice Monitoring, Agriculture and Forestry: Hydric Stress, and Fishing Pressure (Table 11). Subsequently, high, medium, and low priority measurements were defined and its weights were assigned according to the use case to evaluate:

$$W_i = \frac{Numerical_{score_i}}{\sum_i^n Numerical_{score_i}}. \quad (3)$$

**Table 9.** Definition of the numerical score for the criteria and result of the weights.

| Instrument Capabilities | Weight | Numerical Score | | |
|---|---|---|---|---|
| | | 1 | 2 | 3 |
| Latency | 19.2% | >3 h | 2–1 h | <1 h |
| Spatial Resolution | 15.4% | >1 km | 1 km | <1 km |
| Revisit time | 15.4% | Revisit time >24 h | Revisit time: 3–24 h | Revisit time <3 h |
| Accuracy | 14.1% | Worse that state of the art | Equal to state of the art | better that state of the art |
| Payload mass | 12.8% | large | mini | nano-micro |
| Payload power Consumption | 12.8% | large | mini | nano-micro |
| Measurements relevance | 10.3% | Low | Medium | High |

**Table 10.** Instrument technologies' attributes and related numerical scores.

| Instrument Capabilities | Numerical Score | | | |
|---|---|---|---|---|
| | 0 | 1 | 2 | 3 |
| Latency | N/A | high | medium | low |
| Spatial Resolution | N/A | worse than required | minimun requirement met | requirement meet or better |
| Swath | N/A | Narrow swath <400 km | Moderate swath <1000 km | Wide swath >1000 |
| Accuracy | N/A | Worse than required | Equal to requirement | Requirement meet or better |
| Payload mass | N/A | large | mini | nano-micro |
| Payload power Consumption | N/A | >150 W | 25–150 W | ≤25 W |
| Data relevance | N/A | Marginal | High | Primary |

**Table 11.** The priority level of the measurement according to the use case priority.

| **Use Case Priority** | **Marine for Weather Forecast** | | **Sea Ice Monitoring** | | **Agriculture and Forestry: Hydric Stress** | | **Fishing Pressure** | |
|---|---|---|---|---|---|---|---|---|
| **Measurements** | **Priority Level** | **Weight [%]** | **Priority Level** | **Weight [%]** | **Priority Level** | **Weight [%]** | **Priority Level** | **Weight [%]** |
| Ocean Surface currents | H | 9.375 | M | 5.000 | L | 3.570 | M | 5.410 |
| Wind speed over sea surface | H | 9.375 | M | 5.000 | L | 3.570 | M | 5.410 |
| Dominant wave direction | H | 9.375 | M | 5.000 | L | 3.570 | M | 5.410 |
| Significant wave height | H | 9.375 | M | 5.000 | L | 3.570 | M | 5.410 |
| Sea Surface temperature | M | 6.250 | H | 7.500 | L | 3.570 | H | 8.110 |
| Atmospheric pressure over sea surface | M | 6.250 | L | 2.500 | L | 3.570 | M | 5.410 |
| Sea ice cover | M | 6.250 | H | 7.500 | L | 3.570 | L | 2.700 |
| Sea ice type | M | 6.250 | H | 7.500 | L | 3.570 | L | 2.700 |
| Sea ice thickness | L | 3.125 | H | 7.500 | L | 3.570 | M | 5.410 |
| Iceberg tracking | L | 3.125 | H | 7.500 | L | 3.570 | M | 5.410 |
| Sea ice drift | L | 3.125 | H | 7.500 | L | 3.570 | L | 2.700 |
| Sea ice extent | L | 3.125 | H | 7.500 | L | 3.570 | L | 2.700 |
| Surface soil moisture | L | 3.125 | L | 2.500 | H | 10.710 | L | 2.700 |
| Ocean chlorophyll concentration | L | 3.125 | L | 2.500 | L | 3.570 | H | 8.110 |
| Ocean imagery and weather leaving radiance | L | 3.125 | M | 5.000 | L | 3.570 | H | 8.110 |
| Color dissolved organic mater | L | 3.125 | L | 2.500 | L | 3.570 | H | 8.110 |
| Estimation of crop evapotranspiration | L | 3.125 | L | 2.500 | H | 10.710 | L | 2.700 |
| Detection of water stress in crops | L | 3.125 | L | 2.500 | H | 10.710 | L | 2.700 |
| Crop growth & condition | L | 3.125 | L | 2.500 | H | 10.710 | L | 2.700 |
| Monitoring system vessels | L | 3.125 | M | 5.000 | L | 3.570 | H | 8.110 |

Priority level and numerical score: L: Low = 1; M: Medium = 2; H: High = 3.

When the instrument score by measurement is defined, the ranking of the instruments is obtained. The instrument ranking (Table 12) is computed as:

$$Ranking_{instrument} = \sum_{i}^{n} (instrument_{score-by-measurement} * W_i). \quad (4)$$

**Table 12.** Ranking results for each technology for each use case.

| Instrument/Technology | Ranking Results [%] | | | |
|---|---|---|---|---|
| | Marine for Weather Forecast | Sea Ice Monitoring | Agriculture and Forestry: Hydric Stress | Fishing Pressure |
| **Multispectral Radiometer** | 21.6 | 23.1 | 30.1 | 31.2 |
| **Hyperspectral Radiometer** | 11.2 | 10.7 | 19.9 | 11.8 |
| **Hyperspectral . Sounder (IR)** | 10.6 | 8.5 | 6.1 | 11.4 |
| **L-Microwave Radiometer** | 8.5 | 10.6 | 19.4 | 8.1 |
| **Ka, K, W-Microwave Radiometer** | 19.3 | 21.6 | 11.2 | 10.4 |
| **GNSS-R** | 39.4 | 29.6 | 24.8 | 25.3 |
| **X-, Ka, K, W-Microwave Radiometer** | 21.2 | 23.7 | 12.1 | 14.6 |
| **Ka-, U-, D-Microwave Sounder** | 5.9 | 2.37 | 3.4 | 5.1 |
| **Automatic Identification System (AIS)** | 3.1 | 5.0 | 3.6 | 8.1 |
| **Radar Scatterometer** | 11.9 | 12.7 | 6.8 | 6.8 |
| **Lidar** | 1.04 | 2.5 | 1.2 | 1.8 |
| **Synthetic Aperture Radar (SAR) Altimeter** | 27.9 | 21.4 | 12.7 | 16.3 |
| **X-SAR Imager** | 30.8 | 32.5 | 18.23 | 23.56 |

In order to evaluate the robustness of the methodology implemented, a sensitivity analysis at 25% has been performed to estimate the impact of the weights over the ranking of the technologies. Figure 3 shows the same trend in the rank of the technologies by varying randomly 100 times all weights at the same time for each use case prioritized. In this model, the priority level of the measurements and the number of measurements that can measure the sensors are the critical parameters to rank the technologies.

When the priority use case is Marine for Weather Forecast, the key technologies in ranked order are GNSS-R, X- band SAR imager, and Radar Altimeter with SAR processing (Table 12, columns 1 and 2). The sensitivity analysis is summarized in Figure 3a. The simultaneously random weights defined a clear trend in each technology. Columns 1 and 3 of the Table 12 shows the relevant technologies when selecting the Sea Ice Monitoring use case as the priority. They are X-band SAR, GNSS-R, X-, K-, Ka-, W-band MWIm, and Radar Altimeter (SAR). Figure 3b presents a similar tendency in the results when the weights are varying randomly.

The valuable technologies for the Agriculture- Hydric stress use case in ranked order are Multispectral sensors, GNSS-R, Hyperspectral, and L-band MW; the same distribution has been found in the sensitivity analysis (Figure 3c). Figure 3d shows the sensitivity analysis of the technology rank when the Fishing Pressure use case is the priority. The most important technology also is the Multispectral sensor.

In general, the prioritized list of the main technologies to ensure that the gaps are covered taking into account the priority level of different use cases in the time frame 2020–2030 are GNSS-R, imaging X-band SAR, with 1 km of spatial resolution, and Multispectral sensor. GNSS-R provides support to marine and land services of Copernicus and can collaborate with other technologies to improve the measurements. SAR can provide several data from the ocean and can collaborate with the land data. The best ranked optical payload to support multiple services of Copernicus program is a Multispectral sensor with bands in the VIS (442.5, 485, 490, 510, 560, 640, 660, 665 nm), NIR (1610 nm), MWIR (3.7, and 4.05 μm) and TIR (8.55, 11, and 12 μm).

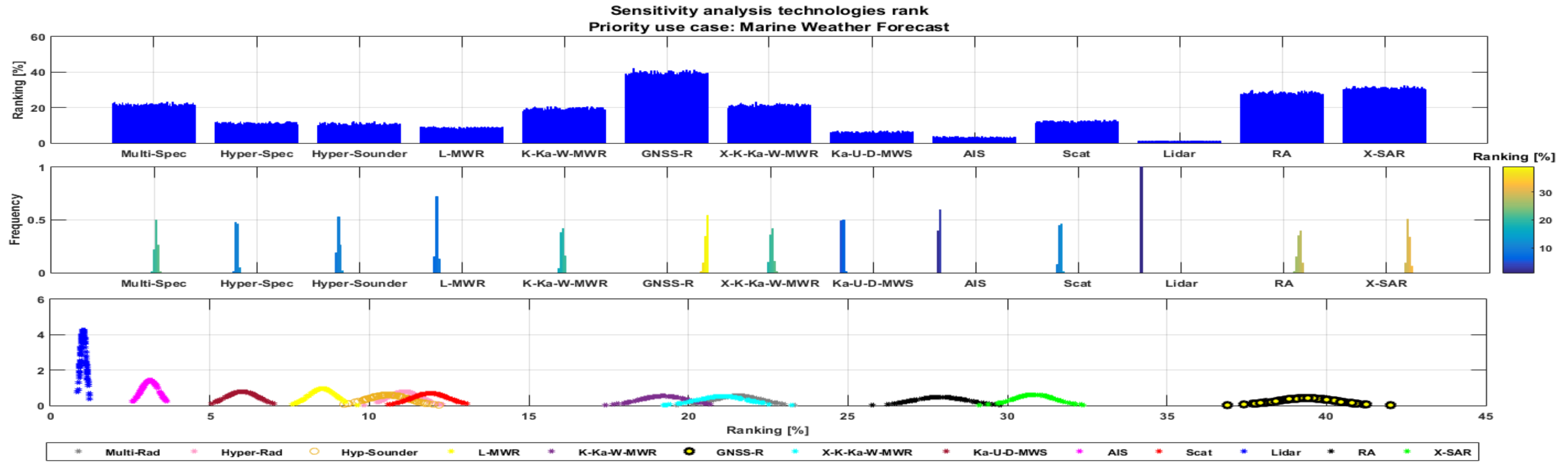


(**a**) High priority: Marine for Weather Forecast use case

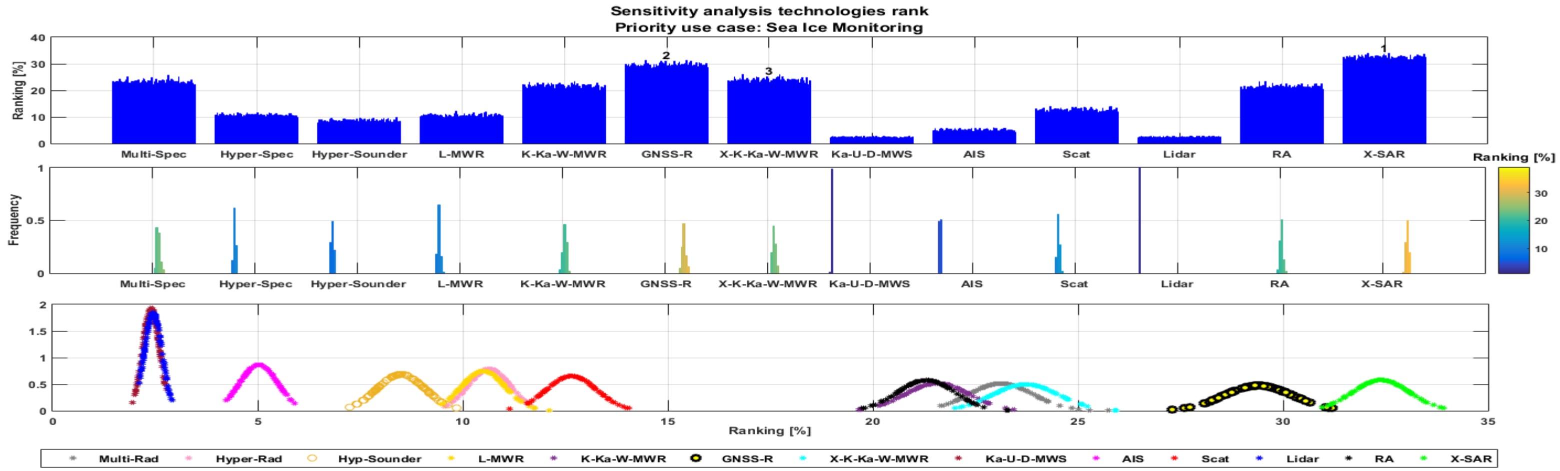


(**b**) High priority: Sea Ice Monitoring use case

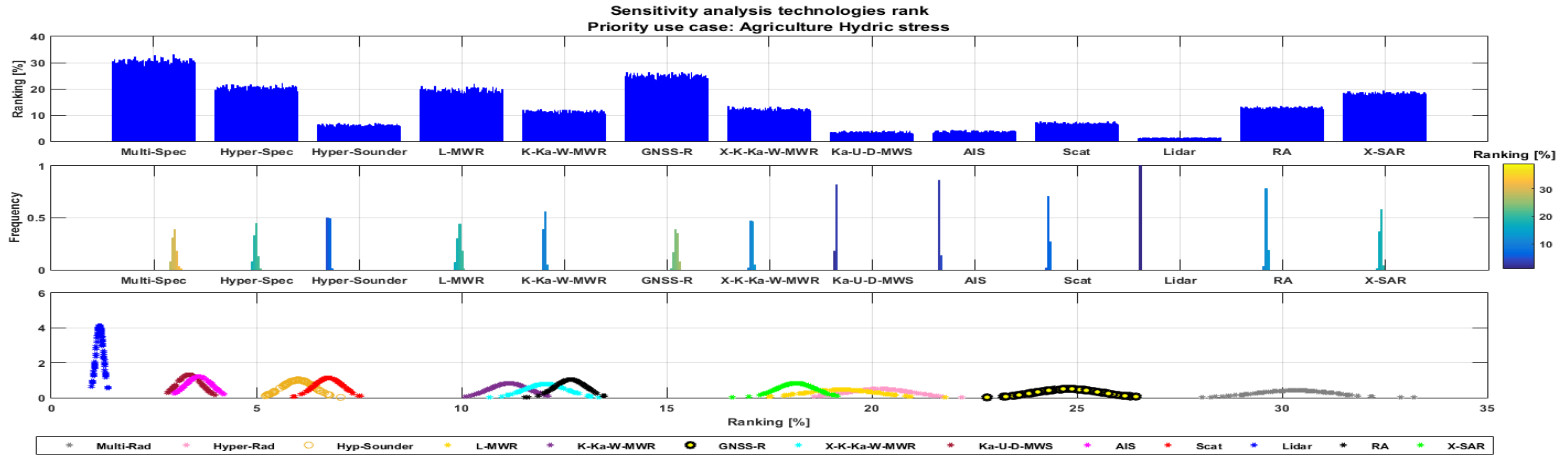


(**c**) High priority: Agriculture- Hydric Stress use case

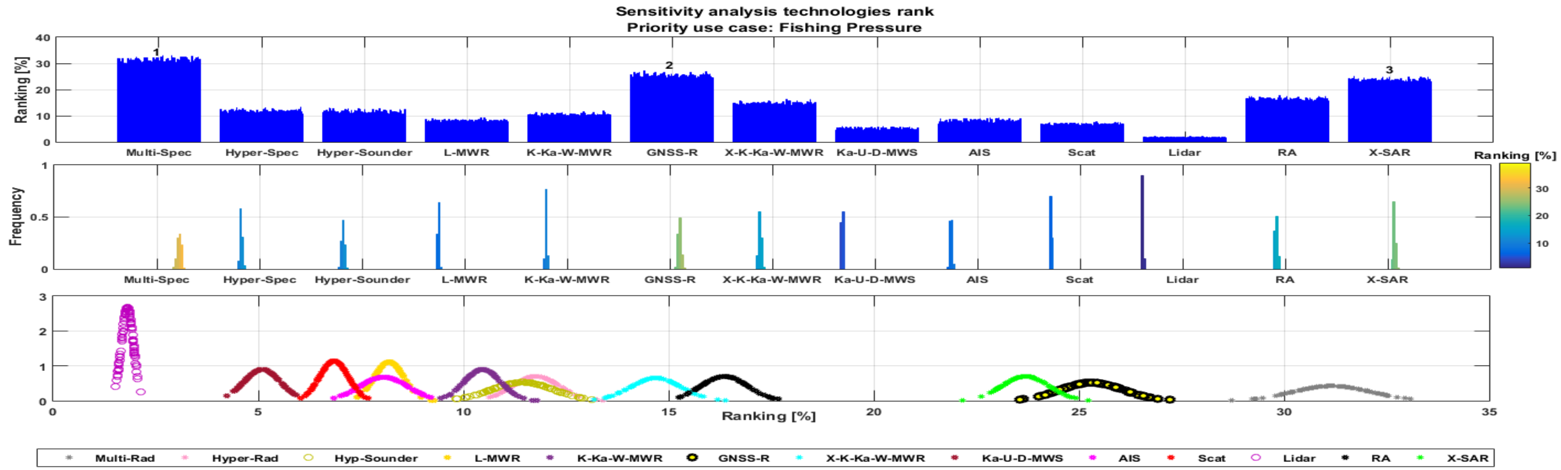


(**d**) High priority: Fishing Pressure use case

**Figure 3.** Sensitivity analysis at 25% for different use cases priorities. (**a**) Marine for Weather Forecast; (**b**) Sea Ice Monitoring; (**c**) Fishing Pressure; (**d**) Agriculture and Forestry: Hydric Stress.

## 7. Conclusions

This study has reviewed the state of the art in EO sensors and platforms and has presented a methodology to select the best instruments' technologies and platforms required to complement the Copernicus system in the time frame 2020–2030. Suitable instruments for small platforms have been analyzed using several attributes, and they have been ranked using a quantitative scoring method. Results show that the most relevant payloads capable of filling the measurements gaps are: GNSS-R at 10 km spatial resolution, X-band imaging SAR at 1 km spatial resolution, and multispectral Optical instrument with bands in the VIS (10 m of spatial resolution), NIR (10 m), MWIR (1 km), and TIR (1 km).

The high temporal resolution of one hour required can only be achieved if a sufficiently large number of spacecrafts are used; then, the architecture selection could be analyzed and optimized [31,71]. A distributed or Federated Satellite System (FSS) will help to reduce the temporal gaps. The possibility to create strategic alliances to establish distributed or federated architectures between different missions and agencies must be carefully evaluated to safe costs. Federated Satellite System (FSS) concepts could also be applied to future instrument technologies to cover the gaps, taking into account different satellites program and space agencies.

**Author Contributions:** E.L. performed the survey of the instruments and commercial platforms; E.L., A.C., H.P., P.R., S.T., J.C. and S.P. identified the potential instruments to cover the measurements gaps; E.L. developed the quantitative method; A.C. revised the quantitative method; E.L. wrote the paper; A.C., H.P., P.R., S.T., J.C. and S.P. revised it.

**Funding:** This project has been funded by the EU H2020 ONION project, under grant agreement 687490. It has also received support from projects AGORA (ESP2015-70014-C2-1-R) of the Spanish Ministry of Economy and Competitiveness, an ICREA Academia Award from the Catalan Government.

**Conflicts of Interest:** The authors declare no conflicts of interest.

## Appendix A

This section presents all the commercial LEO small platforms that have been considered in the survey with their corresponding references. Then, the commercial platforms are assessed in terms mass, power consumption, communications, pointing control, and knowledge. Tables A1–A3 summarize each platform and manufacturer with the available capability to support a wide range of available payload mass and power. These small platforms were categorized into three groups' nano-, micro-, and mini- platforms based on the criteria of the International Academy of Astronautics [110]. Nano-satellites have a mass smaller than 10 kg, micro-satellites have a mass between 10 kg and 100 kg, and mini-satellites have mass in the range from 100 kg to 1000 kg.

**Table A1.** Survey of available nano-satellite platforms for Earth Observation.

| Product | Manufacturer | Total Mass [kg] | Size [cm] | Payload Mass [kg] | Payload Volume | Payload Power [W] | Pointing Control | Pointing Knowledge | Communication Downlink | Propulsion |
|---|---|---|---|---|---|---|---|---|---|---|
| THUNDER (3U) [85] | Space Flight Laboratory | 3.5 | 10 × 10 × 34 | 1 | 1000 $cm^3$ | 1–2 average | 2° | - | S-band 32 kbps–2 Mbps | Cold Gas |
| Endeavour-3U [18] | Tyvak NanoSatellite Technology Inc. | 5.99 | 30 × 10 × 10 | - | 2U | 12 average, 70 peak | 3° | 25 arcsec | UHF, S-band 10 Mbps | Cold gas |
| GRYPHON (GNB) [85] | Space Flight Laboratory | 7 | 20 × 20 × 20 | 2 | 1700 $cm^3$ | 3–4 average, 6 peak | 2° | - | S-band 32 kbps–2 Mbps | Cold gas |
| GOMX 1U [98] | GomSpace ApS | 0.725 | 1U | - | 0.4U | 1.33 average | 10° | 5° | UHF, VHF | - |
| GOMX 2U [98] | GomSpace ApS | 1.2 | 2U | - | 1.4U | 2.48 average | 10° | 5° | UHF, VHF | - |
| GOMX 3U [98] | GomSpace ApS | 1.5 | 3U | - | 2.3U | 9.4 average | 10° | 5° | UHF, VHF, optional X-band | - |
| SMALL SAT 6U [12] | Nexeya | 10 | 10 × 22 × 34 | 3 | - | 7 average, 100 peak | - | - | X-band 100 Mb | Available |
| XB-12 [19] | Blue Canyon Technologies LLC | - | 12U | - | 11U | - | 1 arcsec | 0.002° | UHF, S-band, X-band Up to 15 Mbps | Up to 7 thrusters |
| XB-3 [19] | Blue Canyon Technologies LLC | - | 3U | - | 2U | - | - | - | UHF, S-band, X-band Up to 15 Mbps | Up to 7 thrusters |
| XB-6 [19] | Blue Canyon Technologies LLC | - | 6U | - | 5U | - | 1 arcsec | 0.002° | UHF, S-band, X-band Up to 15 Mbps | Up to 7 thrusters |
| MAI-3000 [17] | Maryland Aerospace | 8 | 10 × 10 × 30 | 3 | 1.5U | 12 average | 0.1° [a] or 1.1° [b] | 0.01° [a] or 1° [b] | S-band Up to 2 Mbps, X-band available. | Compatible with existing 3U launch adapters |

**Table A2.** Survey of available micro-satellite platforms for Earth Observation.

| Product | Manufacturer | Total Mass [kg] | Size [cm] | Payload Mass [kg] | Payload Volume | Payload Power Average/Peak [W] | Pointing Control | Pointing Knowledge | Communication | Propulsion |
|---|---|---|---|---|---|---|---|---|---|---|
| MAI-6000 [23] | Maryland Aerospace | 29 | 10 × 20 × 30 | 12 | 4U | 20 | 0.1° | 0.01° | S-band Up to 2 Mbps and X-band available. | Compatible with existing launch dispensers |
| SN-50 [21] | Sierra Nevada Corporation Space Systems | - | - | 50 | 40 × 40 $^a$ cm | 100 | 0.03° | 0.024° | 3.5 Mbps | Optional green propulsion capability |
| Altair [20] | Millennium Space Systems | - | 30 × 30 × 30 | 50 | - | 90/250 | 20 arcsec | 10 arcsec | S-Band—2 Mbps downlink | - |
| LEOS-30 $^b$ [95] | Berlin Space Technologies GmbH | 30 | 30 × 30 × 50 | 8 | - | 15/60 | - | - | S-Band—2 Mbps downlink | - |
| LEOS-50 $^b$ [95] | Berlin Space Technologies GmbH | 60 | 50 × 50 × 30 | 15 | - | 20/140 | - | - | X-band—100 Mbps downlink | - |
| NEMO [85] | Space Flight Laboratory | 15 | 20 × 30 × 40 | 6 | 8000 cm$^3$ | 45 | 2 | - | S-band 32 kbps–2 Mbps downlink | Cold gas, resistojet, monopropulsion |
| DEFIANT [85] | Space Flight Laboratory | 20–30 | 30 × 30 × 40 | 6–10 | 11,000 cm$^3$ | 45 | 2 | - | 32 kbps–50 Mbps downlink | Cold gas, resistojet, monopropulsion |
| SMALL SAT 12U [12] | Nexeya | 20 | 22 × 22 × 34 | 30 | - | 12/100 | - | - | S-band 2.5 Mbps downlink, 256 kbps uplink, Optional X-band 100 Mbps downlink | Available |
| SMALL SAT 16U [12] | Nexeya | - | 46 × 22 × 22 | 13 | - | 16/150 | - | - | - | Available |
| SMALL SAT 27U [12] | Nexeya | 40 | 35 × 35 × 34 | 25 | - | 30/200 | - | - | - | Available |
| SSTL-12 [22] | Surrey Satellite Technology Limited | 40–75 | 39 × 39 × 47 | Up 45 | 39 × 39 × 37 cm$^3$ | 10–30 | 2° | 0.007° | Up to 160 Mbps (X-band) | Available |
| SSTL-X50 Platform [91] | Surrey Satellite Technology Limited | 75 | - | Up 45 | 53 × 43 × 40 cm$^3$ | 35/85 | 0.07° | 10 arcsec | - | Available |
| SSTL-100 [92] | Surrey Satellite Technology Limited | Up 100 | - | 15 | 32.1 × 30.3 × 24.6 $^c$ cm$^3$ 17.9 × 21.6 × 39 $^d$ cm$^3$ | 24/48 | 2880 arcsec | 2520 arcsec | Up 80 Mbps | Liquefied Butane Gas |
| XB Microsat [19] | Blue Canyon Technologies LLC | 75 | - | - | 45 × 45 × 80 cm$^3$ | - | 0.002° | 1 arcsec | UHF, S-band, X-band Up to 150 Mbps downlink | Up to 7 thrusters |
| BCP-50 [96] | Ball Aerospace Commercial Technologies Corp. | 80 | - | 30 | 30 × 30 × 55 cm$^3$ | 30 $^e$, 100 $^f$ | 0.03°–0.10° | 0.03° | 2 Mbps downlink, | - |
| LEOS-100 $^f$ [95] | Berlin Space Technologies GmbH | 90 | 60 × 60 × 82.5 | 30 | - | 60/140 | - | - | X-band—100 Mbps downlink | - |

$^a$ Height limited by LV Fairing; $^b$ Integrated payload. Carry optical payload; $^c$ Main payload; $^d$ Secondary payload; $^e$ Worse case; $^f$ Best case.

**Table A3.** Survey of available mini-platforms for Earth Observation.

| Product | Manufacturer | Total Mass [kg] | Size [cm$^3$] | Payload Mass [kg] | Payload Volume [cm$^3$] | Payload Power Average/Peak [W] | Pointing Control | Pointing Knowledge | Payload Data [Downlink] | Propulsion |
|---|---|---|---|---|---|---|---|---|---|---|
| NAUTILUS (NEMO-150) [85] | Space Flight Laboratory | Up 150 | 60 × 60 × 60 | Up 70 | Up 108000 | 50/500 | 2° | - | up to 50 Mbps | Cold gas, resistojet, monopropulsion, Hall thruster. |
| DAUNTLESS [85] | Space Flight Laboratory | Up 500 | 100 × 100 × 100 | Up 250 | Up 500000 | 200/1000 | 2° | - | up to 200 Mbps | Cold gas, resistojet, monopropulsion, Hall thruster. |
| SSTL-150 [92] | Surrey Satellite Technology Limited | Up 150 | 60 × 60 × 30 | 50 | 27.95 × 23.15 × 25.25 | 50 average, 100 peak. | 36 arcsec | 25 arcsec | 80 Mbps | Hot gas Xenon resistojet. |
| SSTL-150 ESPA [86] | Surrey Satellite Technology Limited | - | 60 × 60 × 80 | 65 | 47.5 × 50.5 × 21.1<br>41 × 54.7 × 24.4 | 120 | 1 arcmin | 2.5 arcsec | 2 Mbps | Available |
| SSTL-300 [92,93] | Surrey Satellite Technology Limited | 368 | 89.9 × 81.5 × 106.1 | 150 | 27.95 × 23.15 × 25.25 | 140 | 360 arcsec | 72 arcsec | S-Band | Hot gas Xenon resistojet |
| TET-1 [111] | Astro- und Feinwerktechnik Adlershof | 120 | 67 × 58 × 88 | 50 | 460 × 460 × 428 | 20 to 80 average, 160 peak for 20 min | 2 arcmin | 10 arcsec | S-band—2.2 Mbps | - |
| BCP-100 [87] | Ball Aerospace Commercial Technologies Corp. | 180 | 60.9 × 71.1 × 96.5 | 70 | 140,000 | 100–200 | 0.03°–0.10° | 0.03° | 2 Mbps for each payload[a] | Green Propellant, Hydrazine options |
| SN- 200 [94] | Sierra Nevada Corporation Space Systems | Up 355 | - | 200 | - | 200 | 0.1° | 0.05° | 274 Mbps (X-band) | Xenon HET (TacSat), 4.5 |
| SSTL-600 [92] | Surrey Satellite Technology Limited | Up 429 | 190 × 140 × 47.6 | 200 | 90.1 × 90.8 × 26 | 386 average, 450 peak | 605 arcsec | 360 arcsec | 500 Mbps (X-band) | Liquefied butane gas |
| Eagle-1M [90] | Northrop Grumman | - | - | >175 | - | 500 average, 1200 peak. | 0.05° | 90 arcsec | - | 200 m/s modular |
| TET-X [13] | OHB | 120 | 58 × 88 × 67 | 50 | 1700 | Max. 80 , 160 peak for 25 min | - | 10 arcsec | 100 Mbit/s (X-Band) | Micro propulsion system |
| TET-XL [13] | OHB | 200 | 80 × 84.5 × 80 | 80 | 900 | Max. 150 , 460 peak for 25 min. | - | 10 arcsec | 400 Mbit/s (X-Band), or 1.2 Gbit/s (Ka-Band) | Micro propulsion system |
| LEOStar-2 BUS [90] | Northrop Grumman | 150–500 | - | 210–550 | 1,388,000 | up to 2k (optional) | 15 arcsec | 6 arcsec | 2 Mbps (S-Band), 150 Mbps (X-band) | Blowdown monopropellant hydrazine; |
| LEOSTART-500XO [9] | Astrium | 500–1000 | - | 150–600 | - | 250 average, 450 peak | 0.35° | 0.24 deg | 1.6 Mbps (downlink), | Available |
| ELiTeBUS 1000 [10] | Thales Alenia Space | - | - | 350 | 38 × 27.12 × 14.25 | 1000–1500 | 360 arcsec | 22 arcsec | - | Mono-prop (N2H4) |

## Appendix B

This section presents the sensors that have been considered in the survey with their corresponding references.The sensors are assessed in terms mass, power consumption, data rate, and orbit altitude.

**Table A4.** Survey of microwave imagers (MWI).

| Instrument [Mission] | Frequencies Bands [GHz] | Spatial Resolution [km] | Antenna Size [m] | Swath Width [km] | Mass [kg] | Power [W] | Data Rate [kbps] | Orbit Altitude [km] |
|---|---|---|---|---|---|---|---|---|
| Soil Moisture Active and Passive (SMAP) [SMAP] [25,89] | 1.41 | 40 | 6 | 1000 | 356 | 448 | 40,000 | 685 |
| Microwave Imaging Radiometer using Aperture Synthesis (MIRAS) [Soil Moisture and Ocean Salinity (SMOS)] [25,88] | 1.41 | <50 | 4 [a] | 1000 | 355 | 511 | 89 | 755 |
| WindSat (Coriolis) [25] | 6.8, 10.7, 18.7, 23.8, 37 | 39 × 71 to 8 × 13 | 1.83 | 1200 | 341 | 350 | 256 | 838 |
| AMSR (ADEOS-II) [25] | 6.93, 10.65, 18.7, 23.8, 36.5, 50.3, 52.8 and 89 | 3 × 6 to 40 × 70 | 2 | 1600 | 320 | 400 | 130 | 812 |
| AMSR-2 (GCOM) [25] | 6.93, 7.3, 10.65, 18.7, 23.8, 36.5 and 89 | 5 to 50 [b] | 2 | 1450 | 320 | 400 | 130 | 700 |
| AMSR-E (Aqua) [112] | 6.93, 7.3, 10.65, 18.7, 23.8, 36.5 and 89 | 3 × 5 to 35 × 62 | 2.4 | 1450 | 314 | 350 | 874 | 705 |
| Aquarius (SAC-D) [25] | 1.4 GHz | 100 | 2.5 | 390 | 247 | 291 | 5 | 661 |
| MWI (Metop-SG) [25] | 18.7–183.31 (26 channels) | 8 × 13 to 40 × 65 | 0.75 | 1700 | 220 | 250 | 160 | 817 |
| MADRAS (Megha Tropiques) [25] | 18.7, 23.8, 36.5, 89 and 157 | 40 × 60 to 6 × 9 | 0.65 | 1700 | 162 | 153 | 37 | 867 |
| GMI (GPM) [25] | 10.65, 18.7, 23.8, 36.5, 89, 166, 183.31 | 19 × 32 to 4.4 × 7.2 | 1.2 | 850 | 150 | 140 | 25 | 407 |
| TMI (TRMM) [25] | 10.65, 19.35, 21.3, 37, 85.5 | 37 × 63 to 5 × 7 | 0.61 | 790 | 65 | 50 | 8.8 | 402 |
| SSM/I (DMSP) [84] | 19.35, 23.235, 37, 85.5 | 45 × 68 to 11 × 16 | 0.61 | 1400 | 48.5 | 45 | 3.3 | 850 |

The background color in the table indicates the type of platform suitable for the instrument according to the power and mass requirements; Light gray: Micro-platform; Gray: Mini-Platform; [a] 3 arm size; [b] Resolution range for standard products.

**Table A5.** Survey of microwave sounders (MWS).

| Instrument [mission] | Frequencies [GHz] | Spatial Resolution [km] | Antenna Size [m] | Swath Width [km] | Mass [kg] | Power (W) | Data Rate [kbps] | Orbit Altitude [km] |
|---|---|---|---|---|---|---|---|---|
| ATMS (SNPP, JPSS) [25] | 23.8–183 (22 channels) | 16, 32 and 75 | - | 2600 | 75 | 130 | 30 | 824 |
| AMSU-A (NOAA-15/16/17/18/19, Metop A/B/C and Aqua) [25] | 23 to 89 (15 Channels) | 48 | 0.17 and 0.08 [a] | 2100 | 104 | 99 | 3.4 | 817 |
| Tri-band Microwave Radiometer (MiRaTA) [25,32] | 52–58 175–191 203.8–206.8 (10 channels) | - | 0.1 | - | <4.5 | 6 | 10 | 400 |
| Miniature microwave sounder (EON-MW) [33] | 23/31, 50–60/88, 166/183 (22 channels) | 44, 23, 7.5 | 0.11 | 1000 | 5 | 23 | 50 | 505 |

The background color in the table indicates the type of platform suitable for the instrument according to the power and mass requirements: Very light gray: Nano-platform; Light gray: Micro-platform; Gray: Mini-Platform; [a] This instrument has two antennas with different apertures.

**Table A6.** Survey of GNSS-R instruments.

| Available Instruments | Frequencies & Signals | Spatial Resolution [km] | Swath [km] | Mass [Kg] | Power [W] | Data Rate [kbps] | Orbit Altitude [km] |
|---|---|---|---|---|---|---|---|
| SGR-ReSI (TechDemoSat-1 (TDS-1), CYGNSS) [57] | L1 C/A Code (Options: Galileo E1, GPS L2C, Glonass L1, GPS L5, Galileo E5) | 20–50 | 740 | 1.4 [a] | <12 | 200 | 680 |
| GEROS-ISS (GEROS-ISS) [80] | L1 C/A Code (Options: Galileo E1, GPS L2C, Glonass L1, GPS L5, Galileo E5, and QZSS) | 30 | ∼2000 | 376 | 395 | 1200 | 375–435 |
| FMMPL-2 (FSSCAT) [49] | L1 C/A Code (Options: Galileo E1) | 0.3 | ∼350 | 1.5 | >8.0 | 40 | 500–550 |

The background color in the table indicates the type of platform suitable for the instrument according to the power and mass requirements: Very light gray: Nano-platform; Light gray: Micro-platform; Gray: Mini-Platform; [a] Antenna mass doesn't include.

**Table A7.** Survey of Automatic Identification System (AIS) missions.

| Missions | Satellite Mass [kg] | Size | Power Consumption [W] | Launch Date | Payload |
|---|---|---|---|---|---|
| Triton-2/E-SAIL [97] | 100 | 60 × 60 × 70 cm | 100 | 2018 | AIS |
| Norsat-2/SAT-AIS [97] | 1.5 | 51 × 140 × =168 mm | 5 | 2016 | AIS |
| AISSat [25] | 14 | 1 U | 15 | 2013 | AIS |
| [3]CAT-4 [113] | 9 | 6U | 2 | - | AIS + VIS/NIR camera |
| Canx-6 [25] | 6.5 | 2U | 5.6 | 2008 | AIS |
| AISSat 1 [25] | 6 | - | 0.97 | 2010 | AIS |
| AISSat 2 [25] | 6 | - | 0.97 | 2014 | AIS |
| ZACube-2 [25] | 4 | 3U | - | 2017 | AIS + imager |
| AAUSAT-4 [25] | 0.88 | 1U | 1.15 | 2016 | AIS |

The background color in the table indicates the type of platform suitable for the instrument according to the power and mass requirements: Very light gray: Nano-platform; Light gray: Micro-platform.

**Table A8.** Survey of optical radiometer instruments: multispectral and hyperspectral.

| Instrument (Mission) | Classification | Wavelength [μm] | Aperture Size [m] | Spatial Resolution [km] | Swath Width [km] | Mass [kg] | Power [W] | Data Rate [Mbps] | Orbit Altitude [km] |
|---|---|---|---|---|---|---|---|---|---|
| MetImage [a] (MetOp-SG) [25] | Radiometer/ Multispectral resolution | [0.443–13.345] 20 spectral channels | 0.17 | 0.25 to 0.5 or 1 | 2670 | 296 | 465 | 18 | 817 |
| VIIRS [a] (NOAA-20) [25] | Radiometer/ Multispectral resolution | [0.4–12.5] 22 spectral channels | 0.184 | 0.375 to 0.75 | 3000 | 275 | 240 | 5.9 | 825 |
| Modis [a] (Terra/Aqua) [25] | Radiometer/ Multispectral resolution | [0.4–14] 36 spectral channels | 0.178 | 0.25–1 | 2330 | 229 | 162.5 | 6.1 | 705 |
| SLSTR [b] (Sentinel-3) [24,25] | Radiometer/ Multispectral resolution | [0.545–12.5] 11 spectral channels | - | 0.5–1.0 | 1400 | 140 | 100 | 64 | 814.5 |
| OLCI [c] (Sentinel-3) [25] | Radiometer/ Multispectral resolution | [0.55–10.85] 21 spectral channels | - | 0.3 | 1270 | 150 | 124 | 5 | 814.5 |
| AATSR [b] (Envisat) [25] | Radiometer/ Multispectral resolution | [0.4–15] 7 spectral channels | - | 1 | 500 | 101 | 100 | 0.625 | 774 |
| VIRS [b] (TRMM) [25] | Radiometer/ Multispectral resolution | [0.58–12.05] | - | 2 | 833 | 34.5 | 40 | 0.05 | 402 |
| AVHRR/3 [b] (Metop/ NOAA) [25,61] | Radiometer/ Multispectral resolution | [0.58–12.5] 6 spectral channels | 0.21 × 0.295 | 1.1 | 2900 | 33 | 27 | 0.621 | 850 |
| Naomi [b] (SPOT-6/7) [25] | Radiometer/ Multispectral resolution | [0.45–0.89] 5 spectral channels | - | 0.08 | 25 | 18.5 | - | 60 | 695 |
| CHRIS [b] (PROBA-1) [25] | Imager Spectrometer/ Hyperspectral resolution | [0.4–1.05] 63 spectral channels | 0.12 | 0.036 | 14 | 14 | 8 | 1 | 615 |
| COMIS [c] (STSat-3) [25] | Imager Radiometer/ Hyperspectral resolution | [0.4–1.05] 64 spectral channels | - | 30 or 60 | 15 or 30 | 4.3 | 5 | - | 700 |
| HyperScout/ FSSCAT, (3CAT 5/B) [49] | Imager/ Hyperspectral resolution | [0.4–1.0] 45 spectral bands | 0.1 | 0.04 | 164 | 1.1 | 11 | - | 300 |
| CIRC [c] (ALOS-2) [25] | Infrared radiometer | [8–12] Single TIR channel | 0.08 | 200 | 128 | 3 | <20 | - | 640 |

The background color in the table indicates the type of platform suitable for the instrument according to the power and mass requirements: Very light gray: Nano-platform; Light gray: Micro-platform; gray: mini-platform; [a] Instrument affordable for a wide range of geophysical variables, from cloud classification and properties, to aerosol main properties, land surface variables and sea surface variables. [b] Instrument affordable for cloud analysis, aerosol inference, land surface variables and sea surface variables. [c] Instrument affordable for Observation of land surface (e.g., vegetation), marine biology (e.g., ocean color), and cloud/aerosol.

**Table A9.** Survey of optical sounders instruments: multispectral and hyperspectral.

| Instrument (Mission) | Classification | Wavelength [μm] | Aperture Size [m] | Spatial Resolution [km] | Swath Width [km] | Mass [kg] | Power [W] | Data Rate [Mbps] | Orbit Altitude [km] |
|---|---|---|---|---|---|---|---|---|---|
| IASI [b] (MetOp) [25] | Fourier Transform spectrometer b Radiometer/ Hyperspectral resolution | [3.62–15.5] 8461 spectral samples | 1.1 | 25, 1–30 | 2052 | 236 | 210 | 1.5 | 827 |
| AIRS [a] (Aqua) [25] | Infrared sounder/ Hyperspectral resolution | [0.4–15.4] spectral channel >2300 | 0.219 | 13.5, 1 | 1650 | 177 | 220 | 1.27 | 705 |
| CrIS [a] (JPSS) [25] | Infrared Sounder/ Hyperspectral resolution | [3.92–15.38] 1345 spectral channels | 0.8 | 14 | 2200 | 152 | 124 | 1.5 | 824 |
| HIRS/4 [a] (MetOp, NOAA) [25] | Infrared sounder/ Multispectral resolution | [0.69–14.95] 20 spectral channels | 0.15 | 10 | 2160 | 35 | 24 | 0.003 | 850 |
| EON-IR [a] CIRAS [25,62] | Infrared Sounder/ Hyperspectral resolution | [4.08–5.13] 625 channels | 0.15 | 3, 13.5 | 2200 | 2.5 | 15 | 2 | 450–600 |

The background color in the table indicates the type of platform suitable for the instrument according to the power and mass requirements: Very light gray: Nano-platform; Light gray: Micro-platform; gray: mini-platform; [a] Instrument affordable for cloud analysis, aerosol inference, land surface variables and sea surface variables.

**Table A10.** Survey of Radar Altimeter instruments.

| Instrument/Mission | Frequency [GHz] | Antenna Size [m] | Spatial Resolution [km] | Mass [kg] | Power [W] | Data Rate [kbps] | Orbit Altitude [km] |
|---|---|---|---|---|---|---|---|
| Altika/SARAL [25] | 23.8, 36.5, 35.75 | 1 | 10 | 40 | 85 | 43 | 800 |
| SWIM/CFOSAT [25] | 13.58 | 0.9 | - | - | 120 | 50 | 519 |
| Altimeter/SWOT [24] | 5.3, 13.58 | 1.2 | 25 | 70 | 78 | 22.5 | 891 |
| Karin*/SWOT [24] | 35.75 | 5 × 0.25 | 0.05 [a]<br>1 [b] | 300 | 1100 | 320,000 | 891 |
| RA-2/Envisat [24,25] | 3.2, 13.6 | 1.5 | 20 | 110 | 161 | 100 | 774 |
| SSALT/TOPEX- Poseidon [24,25] | 13.65 | 1.5 | 25 | 24 | 49 | - | 1336 |

The background color in the table indicates the type of platform suitable for the instrument according to the power and mass requirements: light gray: micro-platform; gray: mini-platform. * Interferometry; [a] Spatial resolution over land; [b] Spatial resolution over ocean.

**Table A11.** Survey of scatterometer instruments.

| Instrument (Mission) | Frequencies [GHz] | Spatial Resolution [km] | Swath Width [km] | Mass [kg] | Power [W] | Data Rate [kbps] | Orbit Altitude [km] |
|---|---|---|---|---|---|---|---|
| ASCAT (Metop) [25] | 5.255 | 50, 25 and 12.5 | 550 | 260 | 215 | 42 | 817 |
| RapidScat (ISS RapidScat) [24] | 13.4 | 50, 25 and 12.5 | 900 | 200 | 220 | 40 | 407 |
| SCA (Metop-SG-B1/B2/B3) [25] | 5.3 | 17–25 | 550 | 600 | 540 | 5000 | 817 |
| SCAT (CFOSAT) [25,82] | 13.256 | 50, 10 | >1000 | <70 | <200 | 220 | 500 |
| WindRAD (FY-3E/3H) [25] | 5.3 and 13.265 | 20 (C-band), and 10 (Ku-band) | 1200 | - | 265 | - | 836 |

The background color in the table indicates the type of platform suitable for the instrument according to the power and mass requirements: gray: mini-platform; black: large-platform.

**Table A12.** Survey of Radar Altimeter instruments with SAR processing.

| Instrument/Mission | Frequency [GHz] | Antenna Size [m] | Spatial Resolution [km] | Mass [kg] | Power [W] | Data Rate [kbps] | Orbit Altitude [km] |
|---|---|---|---|---|---|---|---|
| SIRAL/Cryosat-2 [24,25] | 13.56 | 1.2 | 15<br>0.25 [a] | 70 | 149 | 24,000 | 717 |
| SRAL/Sentinel-3 [24,25] | 5.3, 13.58 | 1.2 | 20<br>0.3 [a] | 60 | 90 | 12,000 | 810 |
| Poseidon-4/ Sentinel-6 [24] | 5.3, 13.58 | - | 20<br>0.3 [a] | 60 | 90 | 12,000 | 1336 |

The background color in the table indicates the type of platform suitable for the instrument according to the power and mass requirements: light gray: micro-platform; gray: mini-platform. [a] Along track resolution (SAR mode).

**Table A13.** Survey of SAR imager instruments.

| Instrument/ Mission | Frequency [GHz] | Spatial Resolution [m] @ Swath [km] | Mass [kg] | Power [W] | Data Rate [Mbps] | Orbit Altitude [km] |
|---|---|---|---|---|---|---|
| L-band SAR/SAOCOM-2 [24] | 1.275 | 10–100 @ 30–320 | 1500 | - | 300 | 620 |
| X-Band SAR/TSX-NG [24] | 9.65 | 1–16 @ 10–100 | 1230 | 2400 | 680 | 515 |
| SAR/RISAT-1/1A/2 [24] | 5.35 | 1–50 @ 10–220 | 950 | 3100 | 1478 | 546 |
| C-Band SAR/Sentinel-1 [24] | 5.405 | 9–50 @ 80–400 | 880 | 4400 | 600 | 693 |
| SAR (CSA)/RADARSAT [24] | 5.405 | 16–100 @ 20–500 | 705 | 1650 | 105 | 798 |
| SAR RCM/RCM [24] | 5.4 | 3–100 @ 20–500 | 600 | 1270 | - | 592 |
| COSI/KOMPSAT-5 [24] | 9.66 | 1–20 @ 5–100 | 520 | 600 | 310 | 550 |
| Severjanin-M/Meteor-M N2 [25,83] | 9.623 | 400–1000 @ 600 | 150 | 1000 | 10 | 830 |

The background color in the table indicates the type of platform suitable for the instrument according to the power and mass requirements: Gray: mini-platform; black: large-platform.

**Table A14.** Survey of the lidar instruments.

| Type of Lidar | Instrument/ Mission | Wavelength [nm] | Mass [kg] | Power [W] | Data Rate [kbps] | Vertical Spatial Resolution [m] | Swath [m] | Orbit Altitude [km] |
|---|---|---|---|---|---|---|---|---|
| Doppler Lidar | ALADIN/ ADM-Aeolus [25] | 355 | 500 | 840 | 11 | 250 | 50,000 | 405 |
| Backscatter LIDAR | ATLID/ EarthCare [25] | 354.8 | 230 | 320 | 820 | 100 | 100 | 394 |
| | CALIOP/ CALIPSO [25] | 532, 1064 | 156 | 124 | 332 | 30 | 333 | 705 |
| | CATS/ ISS CATS [25] | 355, 532, 1064 | 494 | 1000 | 2000 | 30 | 3500 | 407 |
| LIDAR Altimeter | VCL/ DESDynl [24] | 1064 | 225 | 336 | 800 | 1 | 25,000 | 400 |
| | GEDI-Lidar/ ISS GEDI [24] | 1064.5 | 230 | 516 | 2100 | 25 | 7000 | 407 |
| | ATLAS/ ICESat-2 [24] | 1064 | 298 | 300 | 0.45 | 0.1 | 170 | 478 |
| | GLAS/ ICESat [24] | 532, 1064 | 298 | 300 | 0.45 | 0.1 | 170 | 600 |
| Differential Absorption Lidar (DIAL) | IPDA LIDAR/ MERLIN [24,25] | 1645 | 32.5 | 57 | 150,000 | 100 | 0.1 | 506 |

The background color in the table indicates the type of platform suitable for the instrument according to the power and mass requirements: gray: mini-platform; black: large-platform.

## References


1. Earth Explorer Missions. Available online: https://www.esa.int/Our_Activities/Observing_the_Earth/Earth_Explorers_an_overview (accessed on 19 December 2018).
2. European Space Agency: Two New Earth Explorer Concepts to Understand Our Rapidly Changing World. Available online: https://www.esa.int/Our_Activities/Observing_the_Earth/Two_new_Earth_Explorer_concepts_to_understand_our_rapidly_changing_world (accessed on 19 December 2018).
3. ESA Status Report. Available online: http://www.wmo.int/pages/prog/sat/meetings/ET-SAT-11/documents/ET-SAT-11_Doc_3.4_ESA%20EOP%20%20Status%20Report-%204%20April%202017.pdf (accessed on 19 December 2018).
4. Study to Examine the Socio-Economic Impact of Copernicus in the EU—Report on the Socio-Economic Impact of the Copernicus Programme. Available online: https://publications.europa.eu/en/publication-detail/-/publication/62e30ab0-aa54-11e6-aab7-01aa75ed71a1/language-en/format-PDF/source-search (accessed on 17 December 2018).
5. Matevosyan, H.; Lluch, I.; Poghosyan, A.; Golkar, A. A Value-Chain Analysis for the Copernicus Earth Observation Infrastructure Evolution: A Knowledgebase of Users, Needs, Services, and Products. *IEEE Geosci. Remote Sens. Mag.* **2017**, *5*, 19–35. [CrossRef]
6. Lancheros, E.; Camps, A.; Park, H.; Sicard, P.; Mangin, A.; Matevosvan, I.; Lluch, I. Gaps Analysis and Requirements Specification for the Evolution of Copernicus System for Polar Regions Monitoring: Addressing the Challenges in the Horizon 2020–2030. *Remote Sens.* **2018**, *10*, 1098. [CrossRef]
7. European Space Agency: Sentinels Satellites. Available online: http://www.esa.int/Our_Activities/Observing_the_Earth/Copernicus/Overview4 (accessed on 17 December 2018).
8. European Space Agency: Copernicus Contributing Missions. Available online: https://spacedata.copernicus.eu/web/cscda/missions (accessed on 17 December 2018).
9. Dribault, L.; Durteste, C.; Salvatori, A. LeoStart: Lessons Learnt and Perspectives. Small Satellite Conference. 2013. Available online: https://digitalcommons.usu.edu/smallsat/2000/All2000/22/ (accessed on 17 December 2018).
10. Thales Alenia Space: ELiTeBUS$^{TM}$1000 Platform. Available online: https://www.thalesgroup.com/sites/default/files/asset/document/20161212_pr_elitebus_rsdo_en.pdf (accessed on 7 June 2018).
11. Bowen, J.; Tsuda, A.; Abel, J.; Villa, M. CubeSat Proximity Operations Demonstration (CPOD) mission update. In Proceedings of the IEEE Aerospace Conference Proceedings, Big Sky, MT, USA, 7–14 March 2015. [CrossRef]
12. Nexeya: Small Satellites. Available online: http://www.nexeya.com/solutions/space-systems/nano-satellites/ (accessed on 16 January 2019)
13. OHB System AG: TET the Small Satellites Series. Available online: https://www.ohb-system.de/tl_files/system/images/mediathek/downloads/pdf/OHB_Messe_TET_2014_web.pdf (accessed on 7 June 2018).

14. Small Geostationary Satellite (SGEO) / Telecommunications & Integrated Applications / Our Activities / ESA. Available online: http://www.esa.int/Our_Activities/Telecommunications_Integrated_Applications/Small_Geostationary_Satellite_SGEO (accessed on 7 June 2018).
15. OHB System AG: SmallGeo. Available online: https://www.ohb-system.de/small-geo-luxor-english.html (accessed on 7 June 2018).
16. Sun, D.W.; Ellmers, F.; Winkler, A.; Schuff, H.; Sansegundo Chamarro, M.J. European small geostationary communications satellites. *Acta Astron.* **2011**, *68*, 802–810. [CrossRef]
17. Maryland Aerospace: Platform Products—MAI-3000—3U CubeSat. Available online: https://www.adcolemai.com/3u-cubesat-mai-3000 (accessed on 7 June 2018).
18. Macgillivray, S. Tyvak Nano-Satellite Systems LLC TM Endeavour: The Product Suite for Next Generation CubeSat Mission. Available online: http://mstl.atl.calpoly.edu/~bklofas/Presentations/SummerWorkshop2012/MacGillivray_Endevour.pdf (accessed on 12 June 2018).
19. Blue Canyon Technologies: Spacecraft Buses, Systems & Solutions—XB Spacecraft Buses. Available online: http://bluecanyontech.com/wp-content/uploads/2018/01/DataSheet_XBSpacecraft_11_F.pdf (accessed on 8 June 2018).
20. Millennium Space Systems—Altair Platforms. Available online: http://www.millennium-space.com/platforms.html#altair (accessed on 8 June 2018).
21. Sierra Nevada Corporation (SNC): Spacecraft Systems—SN-50 Nanosat. Available online: http://mediakit.sncorp.com/mediastore/mediakit/sncspace/146/snc's%20spacecraft%20systems%20overview%20brochure_sn-50_low%20res.pdf (accessed on 8 June 2018).
22. Surrey Satellite Technology Ltd.: SSTL-12 Platform—Mission Configurations. Available online: http://www.sst-us.com/downloads/datasheets/us_platform_sstl-12.pdf (accessed on 7 June 2018).
23. Maryland Aerospace: Platform Products—MAI-6000—6U CubeSat. Available online: https://www.adcolemai.com/6u-cubesat-mai-6000 (accessed on 7 June 2018).
24. World Meteorological Organization: Observing Systems Capability Analysis and Review Tool—Space-Based Capabilities. Available online: https://www.wmo-sat.info/oscar/spacecapabilities (accessed on 7 June 2018).
25. Earth Observation Portal Directory: Satellite Missions Database. Available online: https://directory.eoportal.org/web/eoportal/satellite-missions (accessed on 7 June 2018).
26. Zhang, L.; Shi, H.; Wang, Z.; Yu, H.; Yin, X.; Liao, Q. Comparison of Wind Speeds from Spaceborne Microwave Radiometers with In Situ Observations and ECMWF Data over the Global Ocean. *Remote Sens.* **2018**, *10*, 425. [CrossRef]
27. Tauro, C.B.; Hejazin, Y.; Jacob, M.M.; Jones, W.L. An Algorithm for Sea Surface Wind Speed from SAC-D/Aquarius Microwave Radiometer. *IEEE J. Sel. Top. Appl. Earth Obs. Remote Sens.* **2015**, *8*, 5485–5490. [CrossRef]
28. Kaleschke, L.; Tian-Kunze, X.; Maaß, N.; Mäkynen, M.; Drusch, M. Sea ice thickness retrieval from SMOS brightness temperatures during the Arctic freeze-up period. *Geophys. Res. Lett.* **2012**, *39*. [CrossRef]
29. Ricker, R.; Hendricks, S.; Kaleschke, L.; Tian-Kunze, X.; King, J.; Haas, C. A weekly Arctic sea-ice thickness data record from merged CryoSat-2 and SMOS satellite data. *Cryosphere* **2017**, *11*, 1607–1623. [CrossRef]
30. Ivanova, N.; Pedersen, L.T.; Tonboe, R.T.; Kern, S.; Heygster, G.; Lavergne, T.; Sørensen, A.; Saldo, R.; Dybkjær, G.; Brucker, L.; et al. Inter-comparison and evaluation of sea ice algorithms: Towards further identification of challenges and optimal approach using passive microwave observations. *Cryosphere* **2015**. [CrossRef]
31. Araguz, C.; Llaveria, D.; Lancheros, E.; Bou-Balust, E.; Camps, A.; Alarcón, E.; Lluch, I.; Matevosyan, H.; Golkar, A.; Tonetti, S.; et al. Architectural optimization results for a network of Earth-observing satellite nodes. In Proceedings of the 5th Federated and Fractionated Satellite Systems Workshop, Toulouse, France, 2–3 November 2017.
32. Blackwell, W.J. New Small Satellite Capabilities for Microwave Atmospheric Remote Sensing. In Proceedings of the IEEE MTT-S International Microwave Symposium, Honolulu, HI, USA, 4–9 June 2017.
33. Blackwell, W.J.; Pereira, J. *New Small Satellite Capabilities for Microwave Atmospheric Remote Sensing: The Earth Observing Nanosatellite-Microwave (EON-MW)*; American Meteorological Society: Boston, MA, USA, 2016.
34. Carreno-Luengo, H.; Camps, A.; Perez-Ramos, I.; Forte, G.; Onrubia, R.; Diez, R. 3Cat-2: A P(Y) and C/A GNSS-R experimental nano-satellite mission. In Proceedings of the International Geoscience and Remote Sensing Symposium (IGARSS), Melbourne, VIC, Australia, 21–26 July 2013; pp. 843–846. [CrossRef]

35. Semmling, A.M.; Beckheinrich, J.; Wickert, J.; Beyerle, G.; Schön, S.; Fabra, F.; Pflug, H.; He, K.; Schwabe, J.; Scheinert, M. Sea surface topography retrieved from GNSS reflectometry phase data of the GEOHALO flight mission. *Geophys. Res. Lett.* **2014**. [CrossRef]
36. Morris, M.; Ruf, C.S. Determining tropical cyclone surface wind speed structure and intensity with the CYGNSS satellite constellation. *J. Appl. Meteorol. Climatol.* **2017**. [CrossRef]
37. Clarizia, M.P.; Gommenginger, C.P.; Gleason, S.T.; Srokosz, M.A.; Galdi, C.; Di Bisceglie, M. Analysis of GNSS-R delay-Doppler maps from the UK-DMC satellite over the ocean. *Geophys. Res. Lett.* **2009**. [CrossRef]
38. Mashburn, J.; Axelrad, P.; Lowe, S.T.; Larson, K.M. Global Ocean Altimetry with GNSS Reflections from TechDemoSat-1. *IEEE Trans. Geosci. Remote Sens.* **2018**, *56*, 4088–4097. [CrossRef]
39. Clarizia, M.P.; Ruf, C.S.; Jales, P.; Gommenginger, C. Spaceborne GNSS-R minimum variance wind speed estimator. *IEEE Trans. Geosci. Remote Sens.* **2014**, *52*, 6829–6843. [CrossRef]
40. Wang, F.; Yang, D.; Zhang, B.; Li, W. Waveform-based spaceborne GNSS-R wind speed observation: Demonstration and analysis using UK TechDemoSat-1 data. *Adv. Space Res.* **2018**, *61*, 1573–1587. [CrossRef]
41. Camps, A.; Park, H.; Pablos, M.; Foti, G.; Gommenginger, C.P.; Liu, P.W.; Judge, J. Sensitivity of GNSS-R Spaceborne Observations to Soil Moisture and Vegetation. *IEEE J. Sel. Top. Appl. Earth Obs. Remote Sens.* **2016**, *9*, 4730–4742. [CrossRef]
42. Chew, C.; Shah, R.; Zuffada, C.; Hajj, G.; Masters, D.; Mannucci, A.J. Demonstrating soil moisture remote sensing with observations from the UK TechDemoSat-1 satellite mission. *Geophys. Res. Lett.* **2016**, *43*, 3317–3324. [CrossRef]
43. Alonso-Arroyo, A.; Camps, A.; Aguasca, A.; Forte, G.; Monerris, A.; Rudiger, C.; Walker, J.P.; Park, H.; Pascual, D.; Onrubia, R. Improving the accuracy of soil moisture retrievals using the phase difference of the dual-polarization GNSS-R interference patterns. *IEEE Geosci. Remote Sens. Lett.* **2014**, *11*, 2090–2094. [CrossRef]
44. Rodriguez-Alvarez, N.; Bosch-Lluis, X.; Camps, A.; Aguasca, A.; Vall-Llossera, M.; Valencia, E.; Ramos-Perez, I.; Park, H. Review of crop growth and soil moisture monitoring from a ground-based instrument implementing the Interference Pattern GNSS-R Technique. *Radio Sci.* **2011**, *46*. [CrossRef]
45. Larson, K.M.; Braun, J.J.; Small, E.E.; Zavorotny, V.U.; Gutmann, E.D.; Bilich, A.L. GPS Multipath and Its Relation to Near-Surface Soil Moisture Content. *IEEE J. Sel. Top. Appl. Earth Obs. Remote Sens.* **2010**, *3*, 91–99. [CrossRef]
46. Li, W.; Cardellach, E.; Fabra, F.; Rius, A.; Ribó, S.; Martín-Neira, M. First spaceborne phase altimetry over sea ice using TechDemoSat-1 GNSS-R signals. *Geophys. Res. Lett.* **2017**, *44*, 8369–8376. [CrossRef]
47. Alonso-Arroyo, A.; Zavorotny, V.U.; Camps, A. Sea Ice Detection Using U.K. TDS-1 GNSS-R Data. *IEEE Trans. Geosci. Remote Sens.* **2017**, *55*, 4989–5001. [CrossRef]
48. Foti, G.; Gommenginger, C.; Jales, P.; Unwin, M.; Shaw, A.; Robertson, C.; Rosellõ, J. Spaceborne GNSS reflectometry for ocean winds: First results from the UK TechDemoSat-1 mission. *Geophys. Res. Lett.* **2015**, *42*, 5435–5441. [CrossRef]
49. Copernicus Masters: FSSCat—Towards Federated EO Systems. Available online: https://www.copernicus-masters.com/winner/ffscat-towards-federated-eo-systems/ (accessed on 9 June 2018).
50. Castellví, J.; Camps, A.; Corbera, J.; Alamús, R. 3Cat-3/MOTS nanosatellite mission for optical multispectral and GNSS-R earth observation: Concept and analysis. *Sensors* **2018**, *18*, 140. [CrossRef] [PubMed]
51. Park, H.; Pascual, D.; Camps, A.; Martin, F.; Alonso-Arroyo, A.; Carreno-Luengo, H. Analysis of spaceborne GNSS-R delay-doppler tracking. *IEEE J. Sel. Top. Appl. Earth Obs. Remote Sens.* **2014**. [CrossRef]
52. Martín-Neira, M.; D'Addio, S.; Buck, C.; Floury, N.; Prieto-Cerdeira, R. The PARIS ocean altimeter in-Orbit demonstrator. *IEEE Trans. Geosci. Remote Sens.* **2011**, *49*, 2209–2237. [CrossRef]
53. Camps, A.; Park, H.; Valencia I Domenech, E.; Pascual, D.; Martin, F.; Rius, A.; Ribo, S.; Benito, J.; Andres-Beivide, A.; Saameno, P.; et al. Optimization and performance analysis of interferometric GNSS-R altimeters: Application to the PARIS IoD mission. *IEEE J. Sel. Top. Appl. Earth Obs. Remote Sens.* **2014**, *7*, 1436–1451. [CrossRef]
54. Martin-Neira, M. A Passive Reflectometry and Interferometry System(PARIS)- Application to ocean altimetry. *ESA J.* **1993**, *17*, 331–355.
55. Camps, A.; Park, H.; Sekulic, I.; Rius, J.M. GNSS-R altimetry performance analysis for the GEROS experiment on board the international space station. *Sensors* **2017**, *17*, 1583. [CrossRef]

56. Ribo, S.; Arco, J.C.; Oliveras, S.; Cardellach, E.; Rius, A.; Buck, C. Experimental results of an x-band PARIS receiver using digital satellite TV opportunity signals scattered on the sea surface. *IEEE Trans. Geosci. Remote Sens.* **2014**, *52*, 5704–5711. [CrossRef]
57. Surrey Satellite Technology: SGR-ReSI. Available online: http://www.sst-us.com/getfile/e4b5fba3-8d9a-499d-8e50-568ffa156bcd (accessed on 9 June 2018).
58. GOMSpace. GOMspace: Ship Tracking with Space based AIS Receiver. Available online: https://gomspace.com/Shop/payloads/ship-tracking.aspx (accessed on 18 September 2018).
59. Cooley, S.W.; Smith, L.C.; Stepan, L.; Mascaro, J. Tracking dynamic northern surface water changes with high-frequency planet CubeSat imagery. *Remote Sens.* **2017**, *9*, 1306. [CrossRef]
60. Selva, D.; Krejci, D. A survey and assessment of the capabilities of Cubesats for Earth observation. *Acta Astron.* **2012**, *74*, 50–68. [CrossRef]
61. Polar Operational Envoromental Satellites (POES): AVHRR/3. Available online: https://poes.gsfc.nasa.gov/avhrr3.html (accessed on 12 June 2018).
62. Pagano, T.; Abesamis, C.; Andrade, A.; Aumann, H.; Gunapala, S.; Heneghan, C.; Jarnot, R.; Johnson, D.; Lamborn, A.; Maruyama, Y.; et al. Design and development of the CubeSat Infrared Atmospheric Sounder (CIRAS). *SPIE In. Soc. Opt. Eng.* **2017**, *10402*. [CrossRef]
63. Dawson, G.J.; Bamber, J.L. Antarctic Grounding Line Mapping From CryoSat-2 Radar Altimetry. *Geophys. Res. Lett.* **2017**. [CrossRef]
64. Tournadre, J.; Bouhier, N.; Boy, F.; Dinardo, S. Detection of iceberg using Delay Doppler and interferometric Cryosat-2 altimeter data. *Remote Sens. Environ.* **2018**. [CrossRef]
65. Richard, J.; Enjolras, V.; Rys, L.; Vallon, J.; Nann, I.; Escudier, P. Space Altimetry from Nano-Satellites: Payload Feasibility, Missions and System Performances. In Proceedings of the IGARSS 2008, 2008 IEEE International Geoscience and Remote Sensing Symposium, Boston, MA, USA, 7–11 July 2008. [CrossRef]
66. Vogelzang, J.; Stoffelen, A. Scatterometer wind vector products for application in meteorology and oceanography. *J. Sea Res.* **2012**, *74*, 16–25. [CrossRef]
67. Reimer, A.C.; Melzer, B.T.; Kidd, C.R.; Wagner, D.W. Validation of the enhanced resolution ERS-2 scatterometer soil moisture product. In Proceedings of the International Geoscience and Remote Sensing Symposium (IGARSS), Munich, Germany, 22–27 July 2012; pp. 1208–1211. [CrossRef]
68. Brakke, T.W.; Kanemasu, E.T.; Steiner, J.L.; Ulaby, F.T.; Wilson, E. Microwave radar response to canopy moisture, leaf-area index, and dry weight of wheat, corn, and sorghum. *Remote Sens. Environ.* **1981**, *11*, 207–220. [CrossRef]
69. Foster, J.L.; Hall, D.K.; Eylander, J.B.; Kim, E.D.; Riggs, G.A.; Tedesco, M.; Nghiem, S.V.; Kelly, R.E.J.; Choudhury, B.; Reichle, R. Blended Visible, Passive Microwave and Scatterometer Global Snow Products. In Proceedings of the 64th Eastern Snow Conference, St. John's, NL, Canada, 29 May–1 June 2007; pp. 27–36.
70. Belmonte Rivas, M.; Verspeek, J.; Verhoef, A.; Stoffelen, A. Bayesian sea ice detection with the advanced scatterometer ASCAT. *IEEE Trans. Geosci. Remote Sens.* **2012**, *50*, 2649–2657. [CrossRef]
71. Alarcon, E.; Sanchez, A.A.; Araguz, C.; Barrot, G.; Bou-Balust, E.; Camps, A.; Cornara, S.; Cote, J.; Pena, A.G.; Lancheros, E.; et al. Design and optimization of a polar satellite mission to complement the copernicus system. *IEEE Access* **2018**. [CrossRef]
72. Gebert, N.; Domínguez, B.C.; Davidson, M.W.J.; Martin, M.D.; Silvestrin, P. SAOCOM-CS—A passive companion to SAOCOM for single-pass L-band SAR interferometry. In Proceedings of the European Conference on Synthetic Aperture Radar, Berlin, Germany, 3–5 June 2014; pp. 1251–1254.
73. Surrey Satellite Technology Ltd.: NovaSAR-S—The Small Satellite Approach to Synthetic Aperture Radar. Available online: https://www.sstl.co.uk/Downloads/Brochures/115184-SSTL-NovaSAR-Brochure-high-res-no-trims (accessed on 7 June 2018).
74. ICEYE Satellite Missions. Available online: https://www.iceye.com/resources/satellite-missions (accessed on 4 October 2018).
75. Slobbe, D.C.; Lindenbergh, R.C.; Ditmar, P. Estimation of volume change rates of Greenland's ice sheet from ICESat data using overlapping footprints. *Remote Sens. Environ.* **2008**. [CrossRef]
76. Lefsky, M.A.; Harding, D.J.; Keller, M.; Cohen, W.B.; Carabajal, C.C.; Del Bom Espirito-Santo, F.; Hunter, M.O.; de Oliveira, R. Estimates of forest canopy height and aboveground biomass using ICESat. *Geophys. Res. Lett.* **2005**. [CrossRef]

77. Winker, D.M.; Pelon, J.; Coakley, J.A.; Ackerman, S.A.; Charlson, R.J.; Colarco, P.R.; Flamant, P.; Fu, Q.; Hoff, R.M.; Kittaka, C.; et al. The Calipso Mission: A Global 3D View of Aerosols and Clouds. *Bull. Am. Meteorol. Soc.* **2010**. [CrossRef]
78. Illingworth, A.J.; Barker, H.W.; Beljaars, A.; Ceccaldi, M.; Chepfer, H.; Clerbaux, N.; Cole, J.; Delanoë, J.; Domenech, C.; Donovan, D.P.; et al. The earthcare satellite: The next step forward in global measurements of clouds, aerosols, precipitation, and radiation. *Bull. Am. Meteorol. Soc.* **2015**. [CrossRef]
79. Stoffelen, A.; Marseille, G.J.; Bouttier, F.; Vasiljevic, D.; de Haan, S.; Cardinali, C. ADM-Aeolus Doppler wind lidar Observing System Simulation Experiment. *Q. J. R. Meteorol. Soc.* **2006**. [CrossRef]
80. Wickert, J.; Cardellach, E.; Martin-Neira, M.; Bandeiras, J.; Bertino, L.; Andersen, O.B.; Camps, A.; Catarino, N.; Chapron, B.; Fabra, F.; et al. GEROS-ISS: GNSS REflectometry, Radio Occultation, and Scatterometry Onboard the International Space Station. *IEEE J. Sel. Top. Appl. Earth Obs. Remote Sens.* **2016**, *9*, 4552–4581. [CrossRef]
81. Camps, A.J.; Swift, C.T. A two-dimensional Doppler-radiometer for earth observation. *IEEE Trans. Geosci. Remote Sens.* **2001**. [CrossRef]
82. Hauser, D.; Tison, C.; Amiot, T.; Delaye, L.; Mouche, A.; Guitton, G.; Aouf, L.; Castillan, P. CFOSAT: A new Chinese-French satellite for joint observations of ocean wind vector and directional spectra of ocean waves. *Remote Sens.* **2016**, *98780T*, 1–20. [CrossRef]
83. Vnotchenko, S.; Dostovalov, M.; Dudukin, V.; Kovalenko, A.; Musinyants, T.; Riman, V.; Selyanin, A.; Smirnov, S.; Telichev, A.; Chernishov, V.; et al. Wide-swath spaceborne SAR system "Severyanin-M" for remote sensing: First results. In Proceedings of the 9th European Conference on Synthetic Aperture Radar, Nuremberg, Germany, 23–26 April 2012; pp. 422–425.
84. Special Sensor Microwave Imager (SSM/I) | National Snow and Ice Data Center. Available online: https://nsidc.org/data/pm/ssmi-instrument (accessed on 9 June 2018).
85. UTIAS Space Flight Laboratory | Satellite Platforms. Available online: http://www.utias-sfl.net/?page_id=89 (accessed on 14 June 2018).
86. Surrey Satellite Technology Ltd.: SSTL-150 ESPA Satellite Platform. Available online: http://www.sst-us.com/getfile/95b740f8-2873-4943-93e7-97a99655c798 (accessed on 15 June 2018).
87. Ball Aerospace & Technologies Corp.: Ball Configurable Platform (BCP)- 100. Available online: http://www.ball.com/aerospace/Aerospace/media/Aerospace/Downloads/D3072_BCP100-ds_1_14.pdf?ext=.pdf (accessed on 12 June 2018).
88. Camps, A.; Bosch-Lluis, X.; Ramos-Perez, I.; Marchán-Hernández, J.F.; Rodríguez, N.; Valencia, E.; Tarongi, J.M.; Aguasca, A.; Acevo, R. New passive instruments developed for ocean monitoring at the remote sensing lab-Universitat Politècnica de Catalunya. *Sensors* **2009**, *9*, 10171–10189. [CrossRef]
89. Jet Propulsion Labratory: Instrument | Observatory – SMAP. Available online: https://smap.jpl.nasa.gov/observatory/instrument/ (accessed on 8 June 2018).
90. Northrop Grumman: Spacecraft Buses. Available online: http://www.northropgrumman.com/Capabilities/SpacecraftBuses/Pages/default.aspx (accessed on 15 June 2018).
91. Surrey Satellite Technology Ltd.: SSTL-X50 Satellite Platform. Available online: http://www.sst-us.com/downloads/datasheets/sstl-x50.pdf (accessed on 15 June 2018).
92. Abbott, B. Surrey Satellite Technology US LLC. Available online: https://www.sprsa.org/sites/default/files/conference-presentation/2015_06_PayloadHostingBusiness%20Final.pdf (accessed on 14 June 2018).
93. SSTL-300 Satellite Platform. Available online: http://www.sst-us.com/getdoc/e39526e0-8336-4d5d-8d98-7e18f531126d/1353-sstl-300-s1-datasheet.pdf (accessed on 14 June 2018).
94. Sierra Nevada Corporation (SNC): Spacecraft Systems—SN-50 Nanosat. Available online: http://mediakit.sncorp.com/api/document/SN-200_FINAL_web.pdf (accessed on 20 December 2018).
95. Berlin Space Technologies: Small satellite Systems. Available online: https://www.berlin-space-tech.com/products/small-satellite-systems/ (accessed on 7 June 2018).
96. Ball Aerospace & Technologies Corp.: Ball Configurable Platform (BCP)- 50. Available online: http://www.ball.com/aerospace/Aerospace/media/Aerospace/Downloads/D3103_BC__50-ds_0714.pdf?ext=.pdf (accessed on 18 June 2018).
97. Sat-AIS: Satellite-Based Automatic Identification System. Available online: https://esamultimedia.esa.int/docs/telecom/SAT-AIS-factsheet{_}WEB.pdf (accessed on 9 June 2018).
98. GOMSPACE: Platforms. Available online: https://gomspace.com/platforms.aspx (accessed on 18 June 2018).

99. Yan, Q.; Huang, W. Sea ice detection from GNSS-R Delay-Doppler Map. In Proceedings of the 2016 17th International Symposium on Antenna Technology and Applied Electromagnetics, Montreal, QC, Canada, 10–13 July 2016. [CrossRef]
100. Schiavulli, D.; Nunziata, F.; Migliaccio, M.; Frappart, F.; Ramilien, G.; Darrozes, J. Reconstruction of the Radar Image from Actual DDMs Collected by TechDemoSat-1 GNSS-R Mission. *IEEE J. Sel. Top. Appl. Earth Obs. Remote Sens.* **2016**, *9*, 4700–4708. [CrossRef]
101. Camps, A.; Park, H.; Portal, G.; Rossato, L. Sensitivity of TDS-1 GNSS-R Reflectivity to Soil Moisture: Global and Regional Differences and Impact of Different Spatial Scales. *Remote Sens.* **2018**, *10*, 1856. [CrossRef]
102. Van der Schalie, R.; Parinussa, R.M.; Renzullo, L.J.; van Dijk, A.I.; Su, C.H.; de Jeu, R.A. SMOS soil moisture retrievals using the land parameter retrieval model: Evaluation over the mUrrumbidgee Catchment, southeast Australia. *Remote Sens. Environ.* **2015**. [CrossRef]
103. Patilea, C.; Heygster, G.; Huntemann, M.; Spreen, G. Combined SMAP/SMOS Thin Sea Ice Thickness Retrieval. *Cryosphere* **2017**. [CrossRef]
104. Robinson, I.S. *Measuring the Oceans from Space: The Principles and Methods of Satellite Oceanography*; Springer: Berlin/Heidelberg, Germany, 2004; p. 669.
105. Global Sea Ice Concentration Data Record Relase 1.2 (SSMI/SSMIS). Available online: http://www.osi-saf.org/?q=content/global-sea-ice-concentration-data-record-ssmissmis (accessed on 20 December 2018).
106. The Advanced Very High Resolution Radiometer (AVHRR) Multi-Purpose Imaging Instrument Is Used for Global Monitoring of Cloud Cover, Sea Surface Temperature, Ice, Snow and Vegetation Cover Characteristics. Available online: https://www.eumetsat.int/website/home/Satellites/CurrentSatellites/Metop/MetopDesign/AVHRR/index.html (accessed on 19 December 2018).
107. Sentinel-3 Altimetry: Wind Speed. Available online: https://sentinels.copernicus.eu/web/sentinel/user-guides/sentinel-3-altimetry/overview/geophysical-measurements/wind-speed (accessed on 19 December 2018).
108. Sentinel-3 Altimetry: Significant Wave Height. Available online: https://sentinels.copernicus.eu/web/sentinel/user-guides/sentinel-3-altimetry/overview/geophysical-measurements/significant-wave-height (accessed on 19 December 2018).
109. World Meteorological Organization Observational Requirements and Capabilities. Available online: https://www.wmo-sat.info/oscar/requirements (accessed on 21 June 2018).
110. Sandau, R. Status and trends of small satellite missions for Earth observation. *Acta Astron.* **2010**, *66*, 1–12. [CrossRef]
111. Astr-und Feinwerktechnik Adlershof GmbH: TET-1 Platform. Available online: http://www.astrofein.com/2728/dwnld/admin/Brochure_Satellite_TET-1.pdf (accessed on 7 June 2018).
112. AMSR-E Instrument Description | National Snow and Ice Data Center. Available online: https://nsidc.org/data/amsre/amsre-instrument (accessed on 9 June 2018).
113. Castelvi, J.; Lancheros, E.; Camps, A.; Park, H. Feasibility of Nano-Satellites Constellations for AIS Decoding and Fire detection. In Proceedings of the FSS Workshop 2016, Rome, Italy, 10 October 2016; pp. 1–6.


© 2019 by the authors. Licensee MDPI, Basel, Switzerland. This article is an open access article distributed under the terms and conditions of the Creative Commons Attribution (CC BY) license (http://creativecommons.org/licenses/by/4.0/).